

Estimates on the possible annual seismicity of Venus

Iris van Zelst^{1,2}, Julia Maia^{1,3}, Ana-Catalina Plesa¹, Richard Ghail⁴, Moritz Spühler¹

¹Institute of Planetary Research, German Aerospace Center (DLR), Berlin, Germany

²Centre of Astronomy and Astrophysics, Technical University of Berlin, Berlin, Germany

³Université Côte d'Azur, Observatoire de la Côte d'Azur, CNRS, Laboratoire Lagrange, Nice, France

⁴Department of Earth Sciences, Royal Holloway, University of London, Egham, UK

Key Points:

- An inactive Venus with global background seismicity like Earth's continental intraplate seismicity has a few hundred quakes $\geq M_w 4$ per year
- A lower bound on an active Venus where fold belts, coronae, and rifts are seismically active predicts a few thousand quakes $\geq M_w 4$ annually
- The upper bound for an active Venus results in thousands ($\sim 5,000 - 18,000$) venusquakes $\geq M_w 4$ per year

This manuscript is a preprint which has been submitted for publication.

It has not undergone peer review yet.

Subsequent versions of this manuscript may have slightly different content.

If accepted, the final version of this manuscript will be available via the 'Peer-reviewed Publication DOI' link on the right-hand side of this webpage.

Please feel free to contact any of the authors; we welcome feedback!

Corresponding author: Iris van Zelst, iris.vanzelst@dlr.de / iris.v.zelst@gmail.com

15 Abstract

16 There is a growing consensus that Venus is seismically active, although its level of seismicity could be very different from that of Earth due to the lack of plate tectonics. Here, 17 we estimate upper and lower bounds on the expected annual seismicity of Venus by scaling the seismicity of the Earth. We consider different scaling factors for different tectonic 18 settings and account for the lower seismogenic zone thickness of Venus. We find that 95 19 – 296 venusquakes equal to or bigger than moment magnitude (M_w) 4 per year are expected for an inactive Venus, where the global seismicity rate is assumed to be similar 20 to that of continental intraplate seismicity on Earth. For the active Venus scenarios, we 21 assume that the coronae, fold belts, and rifts of Venus are currently seismically active. 22 This results in 1,161 – 3,609 venusquakes $\geq M_w4$ annually as a realistic lower bound 23 and 5,715 – 17,773 venusquakes $\geq M_w4$ per year as a maximum upper bound for an active 24 Venus. 25 26 27

28 Plain Language Summary

29 Venus could be seismically active at the moment, but it is uncertain how many earthquakes (or to use the proper term: venusquakes) there could be in a year. Here, we calculate 30 the minimum and maximum number of venusquakes we could expect in a given year on Venus based on different assumptions. If we assume there is not much seismic 31 activity on Venus (comparable to the interior of tectonic plates on Earth), we find that 32 we could expect about a few hundred venusquakes per year with a magnitude bigger than 33 or equal to 4. For an estimate of the maximum amount of venusquakes, we assume that 34 Venus has regions with more seismic activity: the so-called coronae, fold belts, and rifts. 35 Depending on our assumptions, we then find that more than 17,000 venusquakes could 36 occur in a year with a magnitude bigger than or equal to 4. 37 38

39 1 Introduction

40 After the successful mapping of the Venusian surface by Magellan from 1990 to 1992, 41 for a long time the prevailing hypotheses for Venus’ geodynamic regime were that of a 42 catastrophic or episodic resurfacing regime. The reason for this was the observation of 43 a relatively low number of craters with a near-random spatial distribution on the surface 44 (932 craters; Strom et al., 1994), from which people deduced a uniform, relatively 45 young surface age of 240–800 Myr (McKinnon et al., 1997; Le Feuvre & Wiczorek, 2011). 46 In these catastrophic or episodic resurfacing scenarios, Venus is currently in a relatively 47 quiet tectonic phase after the geologically-recent resurfacing event that led to the observed 48 young surface age (Rolf et al., 2022; O’Rourke et al., 2023). However, the impact 49 crater observations are also consistent with models in which volcanic and tectonic activity 50 occurs at roughly constant rates over time (e.g., Herrick et al., 2023).

51 Indeed, in recent years the view on Venus’ current tectonic activity has shifted towards 52 a more active planet, rivalled in the Solar System only, perhaps, by our own Earth. 53 From a geodynamical point of view, other theories for its geodynamic regime have been 54 put forward, such as the plutonic squishy lid regime (Lourenço et al., 2020), which are 55 consistent with ongoing activity on Venus today. Additionally, the shift towards an active 56 Venus is partly induced by compelling evidence from Magellan, Pioneer Venus, and 57 Venus Express data that Venus might be currently volcanically active. Data from Venus 58 Express shows regions of high thermal emissivity which could be associated with chemically 59 unweathered rocks (Smrekar et al., 2010). The thermal emissivity anomalies correlate 60 with volcanic rises, such as Imdr Regio (Smrekar et al., 2010), indicating geologically 61 recent volcanism in these regions. Depending on the assumption of tectonic regime 62 and amount of volcanic flux, Smrekar et al. (2010) estimate that the bright spots represent 63 recently active volcanoes younger than ~ 2.5 Myr, and potentially as young as

250,000 years or less. Similarly, weathering experiments at Venusian temperature and pressure conditions suggest that the reduction of surface thermal emissivity occurs on time scales of $\sim 500,000$ years (Dyar et al., 2021). Other weathering experiments at Venusian temperatures (but Earth pressures; see M. S. Gilmore et al., 2023, for an overview) have even suggested that this weathering is a rapid process on the order of tens to hundreds of years (Zhong et al., 2023) or even months to years (Filiberto et al., 2020). Additionally, low radar emissivity values, which indicate there is a low amount of high dielectric minerals formed by weathering, typically spatially correspond to the observed thermal emissivity anomalies. Brossier et al. (2022) therefore postulate that these observed low radar emissivity values in Ganis chasma could be the result of volcanic eruptions in the last 30 years, indicating that Venus is volcanically active now (Filiberto et al., 2020). The variability in SO_2 concentration in the clouds observed by Pioneer Venus and Venus Express from 1979 to 2011 has also been attributed to recent volcanic eruptions (Marcq et al., 2013). The most compelling evidence for active volcanism on Venus to date comes from Herrick and Hensley (2023) and Sulcanese et al. (2024), who observed changes in three different volcanic regions by analysing consecutive radar images acquired by Magellan. They interpreted these changes as new volcanic flows and hence ongoing volcanic activity on Venus. In addition, recent gravity and topography analysis indicate that Venus has a thin low viscosity zone which could be interpreted as an indication of partial melting in the mantle (Maia et al., 2023). In line with that, recent estimates from scaling the volcanism of Earth to Venus yield 12 – 42 volcanic eruptions on Venus in a year, depending on assumptions on the amount of volcanism associated with plume-induced subduction at coronae (Byrne & Krishnamoorthy, 2022; Van Zelst, 2022). Future missions such as VERITAS (Smrekar et al., 2020) and EnVision (Ghail et al., 2016) will provide better constraints on Venus’ volcanic activity (Widemann et al., 2023, and references therein).

In the meantime, since Venus seems to be geologically active, it is reasonable to assume that it is also seismically active. Indeed, its seismicity could be more extensive than that of Mars and the Moon, which are both believed to be significantly less tectonically active than Venus (Stevenson et al., 2015). On these bodies, despite being in a stagnant lid regime, seismicity has been observed with the successfully deployed Apollo Lunar Surface Experiments Package on the Moon (Nakamura et al., 1982) and on Mars with the InSight mission (Banerdt et al., 2020). As Venus is now thought to be in a more tectonically active geodynamic regime than a stagnant lid (Rolf et al., 2022), its potential seismicity is thought to be at least comparable with Earth’s intraplate seismicity (Stevenson et al., 2015; Tian et al., 2023; Ganesh et al., 2023). On top of that, observed rift systems (Ivanov & Head, 2011), fold belts (Byrne et al., 2021), wrinkle ridges (Sabbeth et al., 2023b), and coronae (Davaille et al., 2017; Gülcher et al., 2020) could still be actively deforming at present and hence be potentially seismically active. There are even speculations that the Venera 14 lander recorded microseisms from far-away seismicity in the active Beta Regio on Venus, although there are many other potential explanations for these recorded signals (Ksanfomaliti et al., 1982).

Besides a large variety of tectonic features with potential Earth analogues, the crust of Venus has properties similar to the Earth’s crust. Considering their similarities is important when assessing if seismicity might be governed by the same processes and therefore manifest in the same manner in the two planets. Direct compositional measurements from the Soviet landers have shown that the surface of Venus has a similar composition to that of mid-oceanic ridge basalts on Earth (e.g., Abdrakhimov & Basilevsky, 2002). Moreover, the average crustal thickness of Venus has been estimated to be approximately 15 – 20 km (James et al., 2013; Maia & Wiczorek, 2022), which is comparable to the thickness of Earth’s oceanic crust. Considering these similarities, it is reasonable to use Earth’s seismic activity as a starting point to better understand the level of seismicity expected for Venus.

117 Here, we estimate upper and lower bounds of the amount of seismicity that could
 118 be expected for an active Venus, as well as an inactive Venus with seismicity reminis-
 119 cent of intraplate seismicity on Earth. By scaling the seismicity of the Earth to Venus
 120 in Section 2 for different tectonic settings, i.e., using the same philosophy as Byrne and
 121 Krishnamoorthy (2022) that Earth analogues can be applied to Venus, we obtain our re-
 122 sults (Section 3). We then discuss our assumptions and the likely differences between
 123 the seismicity on Earth and Venus, caused by, e.g., their different lithospheric temper-
 124 ature structures, water content, and hence overall lithospheric strength structure, in Sec-
 125 tion 4. In this section, we also discuss and compare with seismicity estimates of previ-
 126 ous studies and comment on how the actual seismicity of Venus could be determined in
 127 the future. This is followed by our conclusions in Section 5.

128 2 Methods

129 In order to estimate the seismicity of Venus, we use a global earthquake catalogue
 130 for Earth and sort the earthquakes into different tectonic areas on the globe, thereby ob-
 131 taining an effective ‘seismicity density’ for each tectonic setting. This ‘seismicity den-
 132 sity’ is defined as the number of quakes per year per km² for each tectonic setting. Hence,
 133 it is effectively the averaged regional *b*-value per km². We then apply this same seismic-
 134 ity density to analogous Venusian settings to obtain three different possible estimates
 135 of Venus’ current seismicity: an estimate for an inactive Venus and an upper and lower
 136 bound for an active Venus, depending on the assumptions that we make. In this section,
 137 we present our methods in detail.

138 2.1 Tectonic settings on Earth

139 To obtain the seismicity density of different tectonic settings on Earth, we calcu-
 140 late the area of seven different tectonic settings on the Earth. For this, we use the re-
 141 cent maps of global geological provinces and tectonic plates from Hasterok et al. (2022).
 142 We define subduction and collision zone areas according to the zones of deformation de-
 143 fined by Hasterok et al. (2022), as the location of the seismicity associated with these
 144 types of plate boundaries typically encompasses a large, diffuse area. We extend the de-
 145 formation zones of Hasterok et al. (2022) to account for deep earthquakes associated with
 146 subduction zones that lie outside of the deformation zones defined at the surface of the
 147 Earth. We further define the areas of transform and strike-slip regions, rift zones, and
 148 mid-oceanic ridges according to the mapping of Hasterok et al. (2022) by defining a 150 km
 149 wide band on either side of the respective plate boundary and correcting for overlapping
 150 areas. The remaining surface area of the Earth is divided into oceanic intraplate and con-
 151 tinental intraplate regions, according to the mapped oceanic and continental crust by
 152 Hasterok et al. (2022). Hence, the surface area of the Earth is divided into seven distinct
 153 (non-overlapping) tectonic settings: subduction zones (5.13% of Earth’s surface area),
 154 collision zones (2.23%), transform and strike-slip regions (3.03%), rift zones (2.17%), mid-
 155 oceanic ridges (4.70%), and oceanic (50.44%) and continental intraplate (32.30%) regions
 156 (Figure 1a, Table S1).

157 2.2 Seismicity of the Earth

158 We use the global Centroid Moment Tensor (CMT; Dziewonski et al., 1981; Ek-
 159 ström et al., 2012) earthquake catalogue from 1976 – 2020 with a completeness magni-
 160 tude of $M_w 5$ to characterise Earth’s annual seismicity. There are various methods to con-
 161 vert seismic moment M_0 (in N m) into moment magnitude M_w (e.g., Stein & Wysession,
 162 2009; Beroza & Kanamori, 2015). Throughout our study, we follow Beroza and Kanamori
 163 (2015) by using the following expression:

$$\log M_0 = 1.5M_w + 9.05. \quad (1)$$

164 We sort the earthquakes of the CMT catalogue in the predefined tectonic areas (Figure 1b)
 165 and obtain an earthquake size-frequency distribution for the different tectonic settings
 166 (Figure 1c). The seismicity density for each of the tectonic settings found on Earth is
 167 then calculated by dividing the earthquake size-frequency distribution by the surface area
 168 (Figure 1d; Table S1).

169 Subduction zones have the highest seismicity density, followed by the other plate
 170 boundary settings and the overall global seismicity density of the Earth (Figure 1d). The
 171 seismicity density of collision zones and strike-slip regions are similar, with a slightly lower
 172 seismicity density for the rift zones. Intraplate seismicity clearly has the lowest seismic-
 173 ity density (approximately one order of magnitude less than the global seismicity den-
 174 sity) with the continental intraplate seismicity density being slightly higher than the oceanic
 175 intraplate seismicity density.

176 2.3 Tectonic settings on Venus

177 For Venus, we consider three different tectonic settings in this study: Venusian rifts
 178 (chasmata), fold belts characterised by compressional deformation, and the volcano-tectonic
 179 corona features, for which we show representative examples in Figure 2 and their dis-
 180 tribution on the surface of Venus in Figure 3a. For each of these tectonic settings, we
 181 assign plausible, potential Earth analogues to obtain an estimate of the potential annual
 182 seismicity of Venus. We refrain from explicitly including other tectonic settings found
 183 on Venus, such as tesserae and wrinkle ridges, because they do not have clear Earth ana-
 184 logues, which makes their seismicity density unconstrained in our methodology. On bod-
 185 ies that are generally considered to be in the stagnant lid geodynamical regime, like Mars
 186 (e.g., Golombek et al., 1992; Knapmeyer et al., 2006) and the Moon (e.g., Williams et
 187 al., 2019), wrinkle ridges have been successfully used to estimate the background seis-
 188 micity. Wrinkle ridge seismicity has also been considered for Venus, with Sabbeth et al.
 189 (2023b) estimating the potential seismicity of wrinkle ridges based on mapped fault lengths,
 190 which we discuss in detail in Section 4. Here, we instead consider the area of Venus out-
 191 side the mapped rifts, fold belts, and coronae as an intraplate tectonic setting (Figure 3a),
 192 thereby implicitly assigning intraplate-like seismicity densities to tectonic settings like
 193 wrinkle ridges and tesserae.

194 2.3.1 Rift zones

195 Rifts on Venus are typically defined as large, broad structural units of 100 km or
 196 more that are characterised by closely-spaced extensional structures (Price & Suppe, 1995;
 197 Ivanov & Head, 2011). They are similar to the so-called groove belts on Venus, which
 198 are smaller and typically contain less dense faulting patterns (Ivanov & Head, 2011). The
 199 extensional features in rift zones are often interpreted as normal faulting and horst-and-
 200 graben structures, which are typically associated with continental rifting on Earth (Foster
 201 & Nimmo, 1996). Indeed, many studies have pointed out both the morphological sim-
 202 ilarity and the similar amount of crustal extension between rifts on Venus and continen-
 203 tal rifts on Earth (e.g., McGill et al., 1981; Phillips et al., 1981; Stoddard & Jurdy, 2012).

204 For example, Foster and Nimmo (1996) provide a detailed comparison between the
 205 East African Rift system on Earth and the rift systems of Beta Regio on Venus. They
 206 identified many similarities, including maximum fault segment lengths, and concluded
 207 that differences stem from the lack of sediment and larger fault strength on Venus. As
 208 another example, Graff et al. (2018) suggested that the rift morphologies of Venus could
 209 be analogous to the Atlantic Rift System prior to ocean opening.

210 Modelling studies also indicate that continental rifting is a plausible mechanism
 211 to generate the rifting morphologies observed on Venus (Regorda et al., 2023). It is clear,
 212 however, that the difference in surface conditions between Venus and Earth plays a role
 213 in the rift mechanism as well (Regorda et al., 2023).

214 The physical mechanisms governing the formation of rifts on Venus are still largely
 215 unclear. In general, Venusian rifts are commonly associated with regions suggested to
 216 be surface expressions of active mantle plumes, such as Atla, Beta, and Phoebe Regiones
 217 (Stofan et al., 1995; Kiefer & Peterson, 2003). As such, continental rifting on Earth could
 218 be a reasonable analogue for rifts on Venus. However, considering Venus’ basaltic crustal
 219 composition — potentially more similar to Earth’s oceanic crust than its continental
 220 crust (Head, 1990) — and increased surface temperature, the rifts on Venus might also
 221 bear resemblance to the mid-oceanic ridges on Earth. Indeed, the three largest rift sys-
 222 tems on Venus, Parga Chasma, Hecate Chasma, and Dali-Diana Chasma, are not typ-
 223 ically associated with hotspots, so the mid-oceanic ridges on Earth might be the best
 224 analogy for these settings on Venus.

225 **2.3.2 Fold belts**

226 There are several different types of compressional structures on the surface of Venus,
 227 including ridges, ridge belts (defined as closely-clustered ridges; Frank & Head, 1990),
 228 and mountain belts (Price & Suppe, 1995). Here, we specifically focus on fold belts, de-
 229 fined by Price et al. (1996) as concentrated zones of compressive deformation forming
 230 linear ridge belts analogous to terrestrial fold-and-thrust belts. As such, the mapping
 231 of fold belts by Price et al. (1996) also includes distinctly compressive regions, such as
 232 the mountain belt of Ishtar Terra. The various compressive features on Venus typically
 233 resemble each other, but differ in terms of topography (Ivanov & Head, 2011). The ori-
 234 gin of these compressional features has been debated, with early studies proposing early
 235 stage mantle downwellings as a mechanism (Zuber, 1990). More recently, Byrne et al.
 236 (2021) suggested that compressional zones like fold belts bound the globally fragmented
 237 crustal blocks in the Venus lowlands and could potentially facilitate movements of the
 238 blocks with respect to each other. The timing of the motion of these crustal blocks is
 239 hard to constrain (Byrne et al., 2021). Potentially these crustal blocks are still moving
 240 to this day, which could imply that the fold belts are still actively deforming at present.
 241 Here, we consider continental collision as the most appropriate analogue for fold belts
 242 on Venus (Phillips & Malin, 1984; Jull & Arkani-Hamed, 1995; Romeo & Turcotte, 2008).

243 **2.3.3 Coronae and corona-like features**

244 Coronae are roughly circular structures characterised by an annulus of high deforma-
 245 tion (Solomon et al., 1991; Basilevsky & Head, 1997; Grindrod & Hoogenboom, 2006;
 246 Ivanov & Head, 2011). Their typical topographic rims typically overlap with their frac-
 247 ture annuli (Sabbeth et al., 2024), which could still be seismically active today (Schools
 248 & Smrekar, 2024).

249 Coronae are unique to Venus and their formation is typically associated with vol-
 250 canism and mantle upwellings (Stofan et al., 1992; Smrekar & Stofan, 1997). There are
 251 various topographic signatures associated with coronae, which have been linked to dif-
 252 ferences in formation mechanisms and stages of formation (e.g., Smrekar & Stofan, 1997;
 253 Gülcher et al., 2020). This variety in topographic signatures of coronae has inspired a
 254 variety of proposed formation mechanisms for coronae including mantle plumes (Smrekar
 255 & Stofan, 1999; Schools & Smrekar, 2024), hot spots (Stofan et al., 1991), and small-scale
 256 upwellings (Squyres et al., 1992; Koch & Manga, 1996; Herrick, 1999; Johnson & Richards,
 257 2003; Musser Jr & Squyres, 1997) followed by gravitational relaxation of isostatically un-
 258 compensated plateaus (Janes et al., 1992) and associated delamination (Smrekar & Sto-
 259 fan, 1997); magmatic loading of the crust due to transient mantle plumes (Dombard et

al., 2007); gravitational Rayleigh-Taylor lithosphere instabilities (Hoogenboom & Houseman, 2006); and lithospheric dripping as a result of the interaction between a mantle plume and a rift (Piskorz et al., 2014).

The formation of large coronae, such as Artemis corona, is typically associated with plume-lithosphere interactions where a rising plume impinges on the Venusian lithosphere and causes subduction-like dynamics and delamination at its edges (Schubert & Sandwell, 1995; Gerya, 2014; Davaille et al., 2017; Smrekar et al., 2018; Gülcher et al., 2020; Baes et al., 2021; Gülcher et al., 2023). For example, Gülcher et al. (2020) used 3-D numerical models to show that different corona structures could represent different plume styles and stages of formation with some coronae exhibiting subduction-like lithosphere dripping at their edges. Using these modelling insights and comparing to topographic data of Venus, Gülcher et al. (2020) found that 37 of 133 studied coronae (i.e., 27.8%) could be actively forming tectonic structures at present. The remaining coronae that they studied were either deemed to be inactive (26.3%) or inconclusive (45.9%) according to the modelled topography profiles. It is worth noting that the coronae studied in Gülcher et al. (2020) are not the complete set of observed coronae on Venus and are instead biased towards the larger corona structures with a diameter ≥ 300 km. Still, their modelling study provides compelling evidence that tectonic processes — and specifically subduction-like processes — could still be active today in a subset of the coronae.

In this study, we mainly follow Gülcher et al. (2020) in assuming that coronae are formed by subduction-like processes associated with plume-lithosphere interactions. Since this is likely only the case for a subset of coronae (e.g., Davaille et al., 2017), we also implicitly consider delamination or plume processes for corona formation (see Section 2.4.2 for more details).

2.3.4 *The surface areas of different tectonic features on Venus*

We calculate the surface area covered by rifts (8.25% of Venus’ surface area; Jurdy & Stoddard, 2007), coronae (7.76%), and fold belts (i.e., compressional regions; 1.64%) from maps by Price and Suppe (1995); Price et al. (1996) as shown in Figure 3a (also see Table S2). We manually ensure that there are no overlapping regions by including rift-associated coronae as part of the rift system. The remaining surface area of Venus that is not assigned an actively-deforming tectonic setting is then considered to be intraplate (82.35% of Venus’ surface; Figure 3a).

2.4 **Scaling from the Earth to Venus**

To scale from the Earth to Venus, we consider several aspects. First, we assign the seismicity density of analogues tectonic settings on Earth (Sections 2.1, 2.2) to the tectonic settings we consider for Venus (Section 2.3). Since this is a seismicity density (i.e., the number of quakes per year per km^2 or the b -value per km^2), we hereby implicitly scale by surface area, taking into account the differences in surface area that tectonic settings occupy on the two planets and the different global surface area between the two planets as a whole. In addition, we scale with the global estimated average seismogenic thickness to account for the fact that Venus most likely has a lower seismogenic thickness than the Earth, because of its higher surface temperature (see Sections 2.4.1, 4.1). Hence, since we consider both the different surface areas and seismogenic thicknesses of the two planets, we actually scale by seismogenic volume when going from Earth analogues to Venus settings. Here, we discuss how we scale the seismogenic thickness of the two planets in detail (Section 2.4.1) and we discuss the Earth analogue assumptions for our three end-member estimates (Section 2.4.2), as well as the possible extent of our seismicity estimates in terms of minimum and maximum quake magnitudes (Section 2.4.3).

308

2.4.1 Seismogenic thickness

309

310

311

312

The seismogenic thickness of a planet’s lithosphere is the maximum depth at which earthquakes can nucleate, typically dictated by the temperature structure of the lithosphere and the location of the brittle-ductile transition. Taken over the entire surface area of the planet, the seismogenic thickness transforms into the seismogenic volume.

313

314

315

316

317

318

319

320

321

322

323

324

325

326

327

328

329

330

331

332

333

334

335

On Earth, the down-dip limit of the seismogenic zone in subduction zones is estimated to range from the 250°C to 550°C isotherms depending on the mineralogy (Tichelaar & Ruff, 1993; Peacock & Hyndman, 1999; He et al., 2007; Scholz, 2019). In a slightly narrower estimate, the down-dip limit of the seismogenic zone is typically associated with the 350°C and 450°C isotherms for megathrust seismicity (Hyndman & Wang, 1993; Hyndman et al., 1997; Gutscher & Peacock, 2003). In order to explain observations of intermediate-depth and deep seismicity in subduction zones and the existence of double seismic zones in subducted slabs, the 600°C and 800°C isotherms are also often cited as the factor limiting seismogenic thickness (Peacock, 2001; Yamasaki & Seno, 2003; Jung et al., 2004; McKenzie et al., 2005; Boettcher et al., 2007; Kelemen & Hirth, 2007; Wang et al., 2017). In high strain rate environments in tectonically active regions, earthquakes have been proposed to occur at temperatures up to 800°C (Chen & Molnar, 1983; Molnar, 2020). There have also been observations of earthquakes in continental lithosphere at depths modelled to correspond with isotherms of 750°C (Prieto et al., 2017) and earthquakes in slabs in regions estimated to exceed 1000°C (Melgar et al., 2018). In hotspot settings, such as Iceland, the average temperature at the base of the seismogenic zone has been estimated to be 750°C with a standard deviation of 100°C (Ágústsson & Flóvenz, 2005). Hence, estimates of the temperature defining the maximum seismogenic zone on Earth vary wildly and depend on the tectonic setting. Depending on the thermal structure of the lithosphere, the estimated seismogenic thickness therefore also carries a large uncertainty. In theoretical and modelling studies, the 600°C isotherm is often assumed to be the end-member temperature for brittle failure, and hence seismogenesis, in Earth’s lithosphere for simplicity (Emmerson & McKenzie, 2007; Van Zelst et al., 2023).

336

337

338

339

340

341

342

343

344

As a measure of the amount of seismicity, the seismogenic thickness is of limited use as it merely defines the region where quakes could nucleate and slip. Indeed, earthquakes can propagate below the seismogenic depth (e.g., Aderhold & Abercrombie, 2016), although they typically nucleate above it, and there are — depending on tectonic setting — vast regions with a significant seismogenic thickness that experience limited seismicity, e.g. the interiors of continental plates, which typically undergo limited deformation. However, despite its limitations, seismogenic thickness is still a useful variable to look at when determining the maximum amount of seismicity that could occur on a given planet.

345

346

347

348

349

350

Since Venus has a higher surface temperature than Earth, assuming the same seismogenic thickness for both planets is likely incorrect. More specifically, we expect Venus to have a lower seismogenic thickness than Earth due to its higher surface temperature and hence shallower brittle-ductile transition in its lithosphere. We therefore need to take the likely difference in seismogenic thickness between the two planets into account when estimating the seismicity of Venus.

351

352

353

354

355

356

357

358

359

In order to estimate the seismogenic thickness scaling factor between Earth and Venus, we first estimate the average seismogenic thickness for the Earth, which is relatively well constrained. For oceanic crust, we assume a representative seismogenic thickness of 36.5 km, which is the depth of the 600°C isotherm (McKenzie et al., 2005; Richards et al., 2018) for the average age of 64.2 Myrs of the oceanic crust (Seton et al., 2020). For an estimate of the average seismogenic thickness of continental crust, we follow Wright et al. (2013), who used coseismic and interseismic observations to arrive at estimates of 14±5 km and 14±7 km of the average continental seismogenic thickness. Regional differences in seismogenic thickness are attributed to compositional differences, differing

360 strain rates, or grain sizes, as Wright et al. (2013) found that there is no clear global re-
 361 lationship between seismogenic thickness and temperature structure for continental crust.
 362 So, following Wright et al. (2013)’s study, we assume an average seismogenic thickness
 363 of 14 km for continental crust in our calculations. Then, applying the ratio of oceanic
 364 to continental crust from Hasterok et al. (2022), we obtain an average seismogenic zone
 365 thickness for the Earth of 26.93 km. We note that this is a lower end-member estimate
 366 of the average seismogenic zone thickness of the Earth, especially since other studies (e.g.,
 367 Molnar, 2020) have found that the seismogenic thickness of continental crust is higher
 368 than the 14 km suggested by Wright et al. (2013). However, for our purpose of obtain-
 369 ing global end-member seismicity estimates with a reasonable uncertainty margin, this
 370 value is adequate to obtain scaling ratios between Earth and Venus as described below.

371 For Venus, we calculate a likely minimum and maximum seismogenic thickness (see
 372 Van Zelst et al., 2024, for the data and scripts used in this study) from proposed end-
 373 member thermal gradients of Venus’ lithosphere (Smrekar et al., 2023; Bjonnes et al.,
 374 2021). Like for our Earth estimate, we calculate the depth corresponding to the 600°C
 375 isotherm, as this seems to limit the seismogenic zone on Earth most robustly. Seeing as
 376 Venus most likely has a drier interior than the Earth that is absent of volatiles, crustal
 377 rocks are stronger compared to their terrestrial counterparts (Mackwell et al., 1998). Hence,
 378 brittle deformation could also occur up to deeper isotherms in Venus’ interior. There-
 379 fore, we also provide seismogenic thickness estimates assuming a temperature of 800°C
 380 as the limiting factor in Van Zelst et al. (2024). However, here, we compute end-members
 381 of the possible annual seismicity on Venus using the 600°C isotherm, as this provides a
 382 better comparison with Earth studies that use the same isotherm value to define the base
 383 of the seismogenic layer. To obtain a minimum estimate of Venus’ seismogenic zone thick-
 384 ness, we calculate the average thermal gradient for Venusian rifts estimated by Smrekar
 385 et al. (2023), which results in a seismogenic thickness of 7.3 km assuming a limiting tem-
 386 perature of 600°C. As a maximum estimate, we use the proposed minimum thermal gra-
 387 dient of 6 K/km for the Mead crater on Venus by Bjonnes et al. (2021), which results
 388 in a seismogenic thickness of 22.7 km for a temperature of 600°C at the base of the seis-
 389 mogenic zone. We note that these estimates represent the thermal gradients during the
 390 formation of the associated features, but given the young ages predicted for Venus’ sur-
 391 face these values are likely representative for its current thermal state.

392 Combining these estimates of the Venusian seismogenic thickness with that of Earth,
 393 we obtain minimum and maximum scaling ratios of 0.27 and 0.84, respectively, to ac-
 394 count for the likely difference in seismogenic thickness between Venus and Earth. We note
 395 that these end-member scaling ratios are a necessary simplification for our global assess-
 396 ment of the potential seismicity on Venus. Future studies could take a more realistic, re-
 397 gional approach, where the seismogenic thickness varies spatially and for different tec-
 398 tonic settings like on Earth.

399 **2.4.2 Three end-member estimates**

400 We consider three different scenarios when scaling the seismicity from the Earth
 401 to Venus (Table S3). First, we consider an inactive Venus where the only seismicity on
 402 the planet is a background seismicity similar to the continental intraplate seismicity on
 403 Earth. This minimum level of seismicity on Venus is a popular hypothesis that has been
 404 used by other studies as well (e.g., Stevenson et al., 2015; Tian et al., 2023; Ganesh et
 405 al., 2023). Here we obtain this estimate by scaling the entirety of Venus with continen-
 406 tal intraplate seismicity on Earth.

407 As a second estimate, we consider an active Venus with conservative assumptions
 408 on its level of activity to provide a lower bound. Following Davaille et al. (2017); Gülcher
 409 et al. (2020); Byrne and Krishnamoorthy (2022), we assume that coronae are surface ex-
 410 pressions of plume-lithosphere interactions with subduction-like features and therefore

411 have a seismic signature similar to that of Earth’s subduction zones. However, for this
 412 lower bound estimate, we do not consider the entire corona area to be active subduction-
 413 like features and associated with the high seismicity density of subduction zones. Instead,
 414 we assume that 27.8% of the area of coronae is active according to Gülcher et al. (2020)
 415 and we only scale this area with subduction zones on Earth. The remaining area of the
 416 coronae is scaled with continental intraplate seismicity on Earth. Hence, we effectively
 417 assume that the corona formation mechanism for the remaining coronae is more akin to
 418 seismicity associated with hot spots or delamination processes on Earth, whose seismic
 419 signatures are implicitly included in our continental and oceanic intraplate seismic den-
 420 sities for Earth. We further assume that the rift zones on Venus have seismicity simi-
 421 lar to (continental) rift zones on Earth (Solomon, 1993; Foster & Nimmo, 1996; Basilevsky
 422 & McGill, 2007; Harris & Bédard, 2015; Graff et al., 2018). The observed fold belts on
 423 Venus that we assume to be compressional features are assumed to have a similar seis-
 424 micity signature to collision zones on Earth. Like the inactive Venus scenario, the remain-
 425 ing area of Venus is scaled according to continental intraplate seismicity on Earth.

426 Our third and last estimate is for an active Venus with the most liberal assump-
 427 tions of plausible tectonic activity on Venus. In this estimate, we assume that all coro-
 428 nae are active, since the amount of active coronae is still highly uncertain (Gülcher et
 429 al., 2020). So, we scale the entire corona area with the subduction seismicity of the Earth.
 430 For the rift zones on Venus, we now scale the seismicity with mid-oceanic ridge seis-
 431 micity on Earth, instead of continental rifting (Graff et al., 2018). Like our lower bound es-
 432 timate for active Venus, we scale the area of fold belts on Venus with collision zones on
 433 Earth and we assume that the rest of the planet is equivalent to continental intraplate
 434 seismicity on Earth.

435 Combining the scaling for the seismogenic zone thickness (Section 2.4.1) with the
 436 three scalings based on the tectonic features allows us to arrive at three different end-
 437 member seismicity estimates for Venus. In short, we obtain the global amount of annual
 438 venusquakes for a certain magnitude $N_{\text{vq}|M_w}$ by applying the following equation:

$$N_{\text{vq}|M_w} = f_{\Delta D} \sum_{\text{tectonic features}} A_{t,V} \cdot \frac{N_{\text{eq},t|M_w}}{A_{t,E}} \quad (2)$$

439 where $f_{\Delta D}$ is the seismogenic zone scaling factor (i.e., 0.27 and 0.84); $A_{t,V}$ is the sur-
 440 face area A of a tectonic feature t on Venus V ; $N_{\text{eq},t|M_w}$ is the number of annual earth-
 441 quakes for a given analogous Earth tectonic feature at a given moment magnitude; and
 442 $A_{t,E}$ is the corresponding surface area of the analogous tectonic feature on Earth. The
 443 sum then indicates a summation over all the tectonic features that are scaled to Venus,
 444 up to and including the intraplate regions, such that we sum over the entire surface area
 445 of Venus. Scaling with the seismogenic thickness as well as the areas of the tectonic set-
 446 tings, effectively allows us to scale by seismogenic volume per tectonic setting to obtain
 447 estimates for Venus’ seismicity (Table S3).

448 **2.4.3 Extrapolating to other magnitudes**

449 In order to actually calculate the potential amount of venusquakes and to extrap-
 450 olate to earthquake magnitudes below the completeness magnitude of $M_w 5$ of the CMT
 451 catalogue, we effectively scale the average slopes of the size-frequency distribution for
 452 the different tectonic settings on Earth (equivalent to $N_{\text{eq},t}$ for all moment magnitudes;
 453 Figure 1c). We specifically assume that the size-frequency distribution of medium-sized
 454 earthquakes with a seismic moment of 10^{17} N m to 10^{19} N m is representative for the
 455 size-frequency distribution of smaller earthquake magnitudes, i.e., the earthquakes fol-
 456 low Gutenberg-Richter statistics (Gutenberg & Richter, 1956; Beroza & Kanamori, 2015).
 457 This assumption allows us to provide estimates of the amount of venusquakes with mo-

458 ment magnitudes of M_w3 and M_w4 . We refrain from reporting on the amount of venusquakes
 459 with lower magnitudes, because they are unlikely to be detected in future seismological
 460 exploration missions of Venus (Krishnamoorthy et al., 2020; Brissaud et al., 2021).

461 Note that this assumption means that we consider the same b -value averaged per
 462 km^2 of the Earth analogues for the different tectonic settings of Venus. Moreover, we as-
 463 sume that this b -value is constant for all quake magnitudes. From seismic catalogues on
 464 Earth, we know this is not necessarily realistic as the frequency of earthquakes with $M_w \geq$
 465 7 starts to drop (Figure 1), although this could also be a result of the limited observa-
 466 tional period of the current seismic catalogues (typically no more than ~ 100 years). Since
 467 there is limited data for Earth on earthquakes with magnitudes $\geq M_w8$, because of their
 468 large recurrence time (Figure 1), calculating the amount of large venusquakes with mag-
 469 nitudes $\geq M_w8$ is less straightforward than extrapolating to smaller quake magnitudes.
 470 In addition, the (potential) maximum quake magnitude on Venus is unknown. One con-
 471 tributing factor is the lower seismogenic thickness of Venus compared to Earth (Section 2.4.1),
 472 which affects the maximum magnitude of quakes and could potentially hint at a smaller
 473 maximum quake size on Venus than on Earth. For these reasons, we do not explicitly
 474 comment on the occurrence of quakes $\geq M_w8$ on Venus in this study, although our method-
 475 ology does provide estimates (i.e., Figure 3). Considering the lower seismogenic thick-
 476 ness of Venus, and hence the smaller potential rupture area, we believe M_w7 venusquakes
 477 to be a reasonable first-order upper bound for our reporting on Venusian seismicity here.

478 3 Results

479 Our results for the different Venus scenarios are summarised in Figure 3 and Ta-
 480 bles 1 and 2, where we list the estimated annual number of quakes for a given moment
 481 magnitude and the global seismicity densities on Venus for our different estimates.

482 3.1 Inactive Venus

483 In our first estimate, we assume that the entirety of Venus can be scaled with the
 484 continental intraplate seismicity of the Earth, so the global estimate and the intraplate
 485 estimate overlap perfectly in Figure 3b. As expected, the amount of seismicity in this
 486 scenario is significantly less than that on Earth with 95 – 296 venusquakes $\geq M_w4$ es-
 487 timated annually, compared to 12,207 earthquakes $\geq M_w4$ per year on Earth. The as-
 488 sociated seismicity density for quakes $\geq M_w4$ lies between $0.21 \cdot 10^{-6}$ and $0.64 \cdot 10^{-6} \text{ year}^{-1} \text{ km}^{-2}$
 489 (Table 2), which is on the same order of magnitude as that of intraplate seismicity on
 490 Earth.

491 3.2 Active Venus - lower bound

492 The lower bound for our active Venus estimate globally predicts more seismicity
 493 than the inactive, intraplate Venus estimate (Section 3.1). The fold belt, rift, and intraplate
 494 tectonic settings on Venus have seismicity on the same order of magnitude in this esti-
 495 mate, as shown by the overlapping bands of seismicity in Figure 3c (also see Figure S1).
 496 The coronae have an order of magnitude more seismicity associated with them, although
 497 only 27.8% of them are assumed to have a subduction-like seismicity density in this es-
 498 timate. Summing up the seismicity of the different tectonic settings results in estimates
 499 of 1,161 – 3,609 venusquakes per year with a moment magnitude $\geq M_w4$ and a seismic-
 500 ity density of $2.52 \cdot 10^{-6}$ to $7.84 \cdot 10^{-6} \text{ year}^{-1} \text{ km}^{-2}$ globally for venusquakes $\geq M_w4$ (Ta-
 501 ble 2). This global seismicity density is significantly less than that of the Earth or any
 502 of its plate boundary settings.

Estimate	$M_w \geq 3.0$	$M_w \geq 4.0$	$M_w \geq 5.0$	$M_w \geq 6.0$	$M_w \geq 7.0$
Inactive Venus	826 - 2568	95 - 296	11 - 34	1 - 4	0 - 0
Active Venus - lower bound	10760 - 33460	1161 - 3609	126 - 391	14 - 42	2 - 5
Active Venus - upper bound	84263 - 262023	5715 - 17773	465 - 1446	44 - 136	4 - 15

Table 1. Number of venusquakes per year equal to or larger than a certain moment magnitude for our three possible Venus scenarios. A range is provided based on the uncertainties in the chosen scaling factor for the seismogenic thickness.

3.3 Active Venus - upper bound

The upper bound of estimated seismicity for an active Venus (Figures 3d, S2) is very close to the annual seismicity observed on Earth, primarily due to the scaling of coronae with Earth’s subduction zone seismicity in this estimate, which also dominates Earth’s seismicity (Figure 1c). Since we scale the rifts on Venus with Earth’s mid-oceanic ridge seismicity in this estimate, we have a different slope for Venusian rift seismicity. This results in an increase in smaller quakes with $M_w \leq 5$. There is no difference between the seismicity expected for the fold belt tectonic setting compared to the lower bound for an active Venus (Section 3.2), as it is scaled in the same way.

Globally, we then estimate 5,715 – 17,773 venusquakes of moment magnitude $\geq M_w 4$, with the upper bound being larger than the number of $M_w \geq 4$ earthquakes estimated for the Earth (12,207). However, note here that this estimate for the number of earthquakes with $M_w \geq 4$ on Earth is an extrapolation of the CMT catalogue, which has a completeness magnitude of $M_w 5$. Therefore, the number of earthquakes $M_w \geq 4$ on Earth is potentially underestimated, leading to similar amounts of estimated seismicity for the upper bound estimate of Venus as on Earth. The seismicity density of quakes $M_w \geq 4$ varies from $12.42 \cdot 10^{-6}$ to $38.62 \cdot 10^{-6}$ year⁻¹ km⁻² (Table 2). This lowest possible seismicity density of quakes $M_w \geq 4$ for an upper bound to our active Venus estimate is slightly lower than the Earth’s seismicity density of quakes $M_w \geq 4$ for continental rift zones ($16.98 \cdot 10^{-6}$ year⁻¹ km⁻²) and the highest possible seismicity density of quakes $M_w \geq 4$ is larger than that of the seismicity density of collision settings on the Earth ($33.62 \cdot 10^{-6}$ year⁻¹ km⁻²) (Table S1).

4 Discussion

In this study, we provide three end-member estimates of possible Venusian seismicity by looking at Earth analogues, following the same philosophy of Byrne and Krishnamoorthy (2022) who previously applied this logic to determine the frequency of volcanic eruptions on Venus. In contrast to Byrne and Krishnamoorthy (2022), we calculate the seismic densities for individual tectonic settings and then scale according to their surface areas and appropriate Earth analogues.

Generally, we estimate that the seismicity of Venus is lower than that of the Earth, except for the most active end-member of Venus activity, which shows seismicity levels similar to that of present-day Earth (Figure 4). At the same time, even the lowest estimate of seismicity for an inactive Venus is larger than the estimated global seismicity of Mars by up to an order of magnitude and of the Moon by several orders of magnitude. The global estimates for these ‘tectonically dead’, stagnant-lid planets are based on extrapolations from measured seismicity by the InSight mission in the case of Mars (Giardini et al., 2020) and analysis of shallow moonquake activity for the Moon (Oberst, 1987) as calculated by Banerdt et al. (2020). This large difference in global seismicity between Mars, the Moon, and Venus is expected even when Venus is tectonically inactive because

542 the difference in size of the planets alone results in significantly less expected events an-
 543 nually for the Moon and Mars. In addition, the Moon and Mars most likely have a much
 544 cooler interior than Venus at present due to their smaller size, again resulting in a less
 545 geologically active body today.

546 There are large differences between the end-member estimates of Venus' seismic-
 547 ity, indicating a range of possible seismic activity on Venus at present, depending on the
 548 many assumptions we are forced to make given the limited amount of data from Venus.
 549 In the following, we discuss the assumptions and limitations of our method and comment
 550 on how our understanding of the seismicity of Venus could increase with upcoming mis-
 551 sions.

552 **4.1 Likely causes of differences between the seismicity on Earth and Venus**

553 Before we assess the individual assumptions we made to obtain our different esti-
 554 mates of Venusian seismicity, it is useful to assess the overarching assumption that Earth's
 555 seismicity can be scaled to Venus.

556 One of the biggest and most straightforward differences between the Earth and Venus
 557 is their different surface temperature. Since temperature plays a crucial role in seismic-
 558 ity through its control on the brittle-ductile transition (Tichelaar & Ruff, 1993; Hynd-
 559 man et al., 1997; Peacock & Hyndman, 1999; Gutscher & Peacock, 2003; Scholz, 2019),
 560 it will have a large effect on the amount of seismicity that can occur. On a global scale,
 561 different surface temperatures can result in different tectonic regimes and deformation
 562 mechanisms (Lenardic et al., 2008; Foley et al., 2012; Weller et al., 2015) which could
 563 greatly change the seismic signatures. In its most extreme case some studies argue that
 564 there will be little to no seismicity on Venus, at least at higher magnitudes (e.g., Karato
 565 & Barbot, 2018). These studies argue that the high surface temperatures on Venus may
 566 exclude the possibility of any kind of substantial seismogenic zone and the unstable slip
 567 mechanisms responsible for earthquakes. Instead, the stresses that are built up in the
 568 Venusian lithosphere could be released through aseismic processes, such as creep (sta-
 569 ble slip) and viscous flow. Karato and Barbot (2018) arrive at this conclusion by assum-
 570 ing a crustal thickness of 30 km based on a global stagnant lid regime and a limit of the
 571 seismogenic zone in the crust at the 400°C isotherm and in mantle at 600°C. However,
 572 recent estimates of the average crustal thickness of Venus are 15 - 20 km (James et al.,
 573 2013; Maia & Wiczorek, 2022). Additionally, strictly separating the mechanical behaviour
 574 of the crust and mantle like this is unrealistic. Instead, a better approach might be to
 575 look at the behaviour of the lithosphere as a whole. For oceanic lithosphere the limit-
 576 ing temperatures for the deepest quakes are the 600 - 800°C isotherms (Chen & Mol-
 577 nar, 1983). Applying these assumptions instead, the method of Karato and Barbot (2018)
 578 does predict a thin seismogenic thickness with the possibility for quakes on Venus.

579 In contrast to this, there are also studies that cite the high surface temperature on
 580 Venus as a potential indirect source of quakes on Venus. Lognonné and Johnson (2015)
 581 mention that the rising surface temperature throughout Venus' evolution could gener-
 582 ate compressive thermoelastic stresses in the crust (Solomon et al., 1999; Dragoni & Pi-
 583 ombo, 2003). This increase in compressive stress could in turn form or activate reverse
 584 faults in Venus' lithosphere. Comparing to the Earth analogues of regions with compres-
 585 sive faulting, Lognonné and Johnson (2015) suggest that these stresses could lead to quakes
 586 with a maximum moment magnitude of 6.5.

587 The difference in surface temperature and hence temperature structure in the litho-
 588 sphere could also change the shear modulus of the Venusian rocks compared to their ter-
 589 ran counterparts. As the seismic moment of a quake depends on the shear modulus of
 590 the rocks, this could alter the magnitudes of quakes on Venus compared to Earth. As
 591 such, it could affect the size-frequency distribution of quakes and hence the b -value.

Estimate	Minimum seismicity density ($\cdot 10^{-6}$ year$^{-1}$ km$^{-2}$)	Maximum seismicity density ($\cdot 10^{-6}$ year$^{-1}$ km$^{-2}$)
Inactive Venus	0.21	0.64
Active Venus - lower bound	2.52	7.84
Active Venus - upper bound	12.42	38.62

Table 2. Estimated minimum and maximum seismicity densities on Venus for quakes $\geq M_w 4$ for three scenarios with different activity-level assumptions.

592 In our estimates, we have taken the difference in surface temperature and its ef-
593 fect on seismicity into account through scaling end-member estimates of the seismogenic
594 thickness of Venus with the average seismogenic thickness of Earth. This implicitly as-
595 sumes that the material properties, including the shear modulus, of rocks on Venus are
596 the same as on Earth. Since the material properties of Venus' (near-)surface rocks are
597 still very unconstrained with the scarce data that is available pointing towards Earth-
598 like mid-oceanic ridge basaltic compositions (e.g., Abdrakhimov & Basilevsky, 2002), we
599 believe this is a reasonable assumption. At the very least, our approach presents a first-
600 order approximation to take the difference in surface temperatures between the two plan-
601 ets into account, although it is by no means a perfect solution that encapsulates the true
602 complexity of the effect of increased surface temperatures on seismicity on Venus.

603 Another important difference between Venus and Earth is likely to be the amount
604 of water available in the crust. On Earth, water plays a vital role, especially in subduc-
605 tion seismicity, with the pore-fluid pressure crucial in determining the stresses in megath-
606 rust settings (Seno, 2009; Angiboust et al., 2012) and dehydration reactions responsi-
607 ble for intermediate-depth and deep seismicity in subduction zones (Green & Houston,
608 1995; Hacker et al., 2003; Jung et al., 2004; Houston, 2015; Wang et al., 2017). This wa-
609 ter is typically added to the subduction system at the outer rise that underlies an ocean
610 in subduction zones (Boneh et al., 2019). On Venus, the amount of water in the litho-
611 sphere is relatively unconstrained (Gillmann et al., 2022; Rolf et al., 2022), with some
612 studies suggesting that Venus is currently relatively dry (Grinspoon, 1993; Namiki & Solomon,
613 1998; Smrekar & Sotin, 2012; Salvador et al., 2022), while others argue that there might
614 still be a significant amount of water in Venus' mantle (Gillmann et al., 2022). This makes
615 it highly uncertain how big a role water could play in the seismicity of Venus. Our es-
616 timates encompass the full spectrum of possible seismicity on Venus with our lower bound
617 using Earth's intraplate seismicity, where water likely plays a smaller role, and our up-
618 per bound including subduction seismicity, where water is an important factor.

619 Strain rates play an important role in seismicity as well, because they determine
620 the time scale of stress build-up and the recurrence time of earthquakes. On Venus, strain
621 rates similar to Earth's active margins have been suggested by R. E. Grimm (1994). How-
622 ever, due to the lack of Earth-like plate tectonics and plate boundaries, there are over-
623 all potentially less large rupture areas, leading to less large-magnitude quakes on Venus.
624 The decreased seismogenic thickness of Venus also plays a role in this by limiting the max-
625 imum rupture area. Although our estimates provide a range of potential venusquakes
626 at large magnitudes (Table 1), it is therefore uncertain if large venusquakes could actu-
627 ally occur. Preliminary mission designs suggest that quake magnitudes of $M_w \geq 3$ could
628 be feasibly observed by a range of plausible seismic detection methods (Krishnamoorthy
629 et al., 2020; Brissaud et al., 2021; Garcia et al., 2024) and our estimates are likely most
630 plausible for this range of seismic magnitude $3 \leq M_w \leq 5$.

631 All in all, there are many uncertainties when it comes to estimating the seismic-
 632 ity of Venus from Earth’s seismicity. Higher resolution data and missions focused on ob-
 633 serving seismicity (discussed in Section 4.3) will help to obtain seismicity estimates for
 634 Venus independent of Earth. However, since those constraints are not yet available, scal-
 635 ing the seismicity of the Earth is a reasonable first-order approximation to gain some in-
 636 sights into the potential seismicity of Venus.

637 4.2 Assumptions in and limitations of our seismicity estimates

638 In order to provide global end-member ranges of the potential seismicity of Venus,
 639 one important simplification that we use is the constant global end-member seismogenic
 640 thickness (see Section 2.4.1). This assumption serves its purpose in that we obtain a range
 641 of plausible seismicity for each end-member estimate, but in reality, the seismogenic thick-
 642 ness will vary laterally across the surface of Venus and depend greatly on, for instance,
 643 the specific tectonic setting. Hence, in order to obtain more regionally-accurate seismic-
 644 ity estimates, future studies should take into account laterally-varying seismogenic thick-
 645 nesses.

646 For our inactive Venus estimate, we assume that the global background seismic-
 647 ity of Venus is similar to the continental intraplate seismicity of the Earth. This is a com-
 648 mon assumption that has also been suggested by e.g., Lorenz (2012); Stevenson et al.
 649 (2015); Byrne et al. (2021); Tian et al. (2023). The number of venusquakes $\geq M_w 4$
 650 per year for this estimate (95 – 296) is also the same order of magnitude as the estimate of
 651 Ganesh et al. (2023), who calculate an estimate of Venus’ seismicity based on the cool-
 652 ing of the planet and the corresponding contraction of the lithosphere and thereby pre-
 653 dict ~ 265 venusquakes $\geq M_w 4$ per year. Lognonné and Johnson (2015) mention that
 654 Stofan et al. (1993) arrive at a slightly higher estimate of 100 quakes $\geq M_w 5$ per year
 655 for intraplate activity with a strain rate of 10^{-19} s^{-1} (R. Grimm & Hess, 1997). In com-
 656 parison, we estimate 11 – 34 quakes $\geq M_w 5$ per year. The reason for this discrepancy
 657 is that Stofan et al. (1993) assume a thicker seismogenic layer (30 km) than we do.

658 Of course, we cannot completely exclude a completely inactive Venus with seismic-
 659 ity densities even lower than our inactive Venus estimate. So, if future missions (Section 4.3)
 660 would find less than 95 quakes $\geq M_w 4$ per year, this would indicate that either the pro-
 661 cesses that are responsible for creating intraplate seismicity on the Earth do not oper-
 662 ate on Venus or the seismic moment release on Venus is fundamentally slower than on
 663 Earth. Physically, this lower seismic activity could for example be caused by the slower
 664 cooling of Venus than previously thought, thereby decreasing the amount of quakes pre-
 665 dicted by Ganesh et al. (2023).

666 For our estimates for an active Venus, we scale the areas of fold belts associated
 667 with compressional deformation on Venus with the seismicity of collision zones on Earth.
 668 We believe this to be a reasonable assumption, considering that Venus’ fold belts and
 669 the Earth analogue are both compressional regimes. The rifts on Venus are scaled with
 670 continental rift seismicity on Earth in the lower bound estimate for an active Venus. This
 671 is also a reasonable assumption, with many studies pointing to the morphological and
 672 geological similarities between the rift zones on Venus and continental rifts on Earth such
 673 as the East African rift zone (Solomon, 1993; Foster & Nimmo, 1996; Kiefer & Swafford,
 674 2006; Basilevsky & McGill, 2007; Stoddard & Jurdy, 2012; Graff et al., 2018; Regorda
 675 et al., 2023). For our upper bound, we scale the rift zones of Venus with mid-oceanic ridge
 676 seismicity since it is also an extensional setting and the higher temperatures at the mid-
 677 oceanic ridges and the corresponding different slope of the size-frequency distribution
 678 on Earth might be a better fit for rift seismicity under Venus’ high surface temperature.
 679 On Earth, the different seismic signatures between continental rifts and mid-oceanic ridges
 680 are not purely temperature-related. Instead, the inherent tectonic differences between
 681 the two settings plays a role as well. Since it is unclear which of these two physical mech-

anisms (or their seismic signatures) best represents the rifting processes on Venus, we believe using one of them for the lower bound estimate and one for the upper bound estimate catches the uncertainty in governing mechanisms in our estimates. For the coronae, we scale with subduction, since multiple studies suggest that coronae, or at least a subset of them, could be the surface expressions of plume-lithosphere interactions with subduction-like features (Davaille et al., 2017; Gülcher et al., 2020; Byrne & Krishnamoorthy, 2022). However, the seismicity associated with this type of plume-lithosphere interactions is uncertain. Assigning the same seismicity density as regular subduction processes on Earth follows Gülcher et al. (2020) and is a reasonable first-order approximation in the absence of other constraints, although the presumable lack of water in coronae and the higher surface temperature will certainly affect its seismic signature as well. Future modelling studies that combine geodynamic modelling with seismic cycle modelling and dynamic ruptures (e.g., van Dinther, Gerya, Dalguer, Mai, et al., 2013; van Dinther, Gerya, Dalguer, Corbi, et al., 2013; van Dinther et al., 2014; Van Zelst et al., 2019) are needed to assess the seismic signatures that could be expected at Venusian coronae. In the interest of providing an upper and lower bound, scaling the coronae by activity is a good first order approximation. However, it is also possible that coronae seismicity does not scale with Earth’s subduction seismicity, but is instead more analogous to, for example, rift or transform fault seismicity, as suggested for the center of Artemis corona (Spencer, 2001). In general though, our upper bound for Venusian seismicity results in seismicity levels slightly higher than, but similar to, that of the Earth, which has also already been suggested previously (e.g., Lorenz, 2012). Choosing a different seismicity density for coronae, such as that of the transform fault setting, would result in a lower amount of estimated venusquakes. Since we are attempting to provide an upper limit to the possible amount of annual venusquakes, our assumption of a subduction seismicity density is reasonable.

Apart from the uncertainty in scaling the chosen tectonic settings correctly, there are also tectonic settings on Venus that we neglect to scale explicitly. For example, we do not explicitly scale the tesserae of Venus with a tectonic setting on Earth, although they are implicitly scaled with the background intracontinental seismicity of the Earth. This is arguably one of the most reasonable assumptions for tesserae, considering that prevailing hypotheses include that they are continental crust analogues (Romeo & Turcotte, 2008; M. Gilmore et al., 2015). We also do not consider the observed extensive regions of wrinkle ridges as seismically active beyond the background intracontinental seismicity of the Earth. A recent study by Sabbeth et al. (2023a) presented a conservative estimate of $9.1 \cdot 10^{16}$ N m to $5.1 \cdot 10^{17}$ N m per year for the annual moment release for wrinkle ridges on Venus based on (low-resolution) mapped fault lengths. Translating this to the size-frequency distributions we use here, Sabbeth et al. (2023a) estimate roughly one venusquake $\geq M_w 4$ every ten years, indicating that the seismicity of wrinkle ridges probably does not significantly contribute to the global seismic budget of the planet. Beyond tesserae and wrinkle ridges, there are also other kinds of deformation structures and potential seismic sources that are not directly considered in this study, such as densely fractured plains, that could also contribute to the seismicity of Venus.

Note that in the estimates presented here, only one type of seismic source is considered, i.e. earthquakes, which by definition are associated with tectonics and volcanism. Other sources such as landslides (Pavri et al., 1992; M. Bulmer & Guest, 1996; M. Bulmer et al., 2006; M. H. K. Bulmer, 2012; Hahn & Byrne, 2023) could be responsible for seismic signals on Venus as well.

4.3 Determining the actual seismicity of Venus in the future

In the next decade, VERITAS (Smrekar et al., 2020) and EnVision (Ghail et al., 2016) will provide a wealth of new data, including high resolution topography, that will provide better constraints on the actual lengths, offsets, and displacements of Venusian

734 faults. This will provide another basis of estimating Venus’ seismicity through scaling
735 relationships applied to surface fault observations (Sabbeth et al., 2023a, 2023b).

736 The new Venus missions will also indirectly provide stronger constraints on the seis-
737 mogenic thickness, which is typically deduced from thermal gradients estimated from stud-
738 ies of the elastic and mechanical lithosphere thickness (e.g. Anderson & Smrekar, 2006;
739 Borrelli et al., 2021; Maia & Wiczorek, 2022; Smrekar et al., 2023) or from impact crater
740 modeling (Bjonnes et al., 2021). These studies rely on the analysis of gravity and topog-
741 raphy data, for which a higher resolution will become available from the VERITAS (Smrekar
742 et al., 2020) and EnVision (Ghail et al., 2016) missions. Estimates of the thermal gra-
743 dient and associated seismogenic thickness could then be obtained with a higher accu-
744 racy and on a more global scale than currently available. They could be included in fu-
745 ture studies of seismicity on Venus and improve on the estimates presented here.

746 Most importantly though, VERITAS will be able to directly measure surface de-
747 formation through Repeat Pass Interferometry (RPI) at 2 cm height precision (Smrekar
748 et al., 2020). Resources permitting, EnVision also hopes to conduct RPI measurements
749 in its extended mission. Besides quantifying movements on the surface of Venus for the
750 first time, both missions will also qualitatively provide insights into which regions are
751 geologically and potentially seismically active.

752 Until the era of new Venus data, we are unfortunately limited by the currently-available
753 datasets. The simplest, first-order estimate of the seismicity of Venus is therefore obtained
754 here through scaling Earth analogues to Venus, without considering individual fault lengths
755 or displacements and detailed seismogenic thickness estimates and instead uses the seis-
756 micity density characteristics of different tectonic settings on Earth.

757 To distinguish between the different scenarios presented in this study and deter-
758 mine how seismically active Venus is, a seismological or geophysical mission to Venus is
759 required to measure seismic signals (Garcia et al., 2024). Although the NASA- and ESA-
760 selected missions to Venus currently do not focus on this, there are promising propos-
761 als to measure Venus’ seismicity in the not-too-distant future. For example, Kremic et
762 al. (2020) presented a mission proposal for a long-duration Venus lander with a seismome-
763 ter on board that can withstand Venus’ high surface temperature. In addition, recent
764 advances in the balloon-detection of earthquakes show great promise for applications to
765 Venus (Garcia et al., 2022; Krishnamoorthy & Bowman, 2023). Our estimates for Venu-
766 sian seismicity may help guide the design of these missions.

767 5 Conclusions

768 We estimate upper and lower bounds on the expected annual seismicity of Venus
769 by scaling the seismicity of the Earth to Venus according to the surface area of differ-
770 ent tectonic settings and the difference in seismogenic thickness between the two plan-
771 ets. Our most conservative estimate is an ‘inactive Venus’, where we assume that the
772 global seismicity of Venus is comparable to Earth’s continental intraplate seismicity. This
773 results in 95 – 296 venusquakes $\geq M_w4$ per year depending on the assumption of seis-
774 mogenic zone thickness. For our active Venus scenarios, we assume that the rifts, fold
775 belts, and coronae on Venus are seismically active. For a lower bound on an active Venus,
776 we then find 1,161 – 3,609 venusquakes $\geq M_w4$ annually, which increases to 5,715 – 17,773
777 venusquakes $\geq M_w4$ for assumptions that constitute our most active Venus scenario.
778 The upper bound of this latter scenario is similar to the seismic activity level of the Earth.
779 Future seismological and geophysical missions could measure the actual seismicity of Venus
780 and distinguish between our three proposed end-members of Venusian seismic activity.
781

Acknowledgements

We warmly thank editor Laurent Montési and reviewers Sue Smrekar, Joseph O'Rourke, and Angela Marusiak who provided thorough and constructive feedback. We also thank two anonymous reviewers who provided feedback on an earlier version submitted to GRL. This research was supported by the International Space Science Institute (ISSI) in Bern, Switzerland through ISSI International Team project #566: Seismicity on Venus: Prediction & Detection. The authors warmly thank the entire ISSI team for fruitful discussions and feedback. IvZ, JM, ACP, and MS additionally acknowledge the financial support and endorsement from the DLR Management Board Young Research Group Leader Program and the Executive Board Member for Space Research and Technology. IvZ also gratefully acknowledges the support by the Deutsche Forschungsgemeinschaft (DFG, German Research Foundation), Project-ID 263649064 - TRR 170.

Author contribution statement

Conceptualization: Iris van Zelst

Data curation: Iris van Zelst, Julia Maia, Richard Ghail, Moritz Spühler

Formal Analysis: Iris van Zelst, Julia Maia

Funding acquisition: Iris van Zelst, Ana-Catalina Plesa

Methodology: Iris van Zelst, Richard Ghail

Supervision: Iris van Zelst

Visualization: Iris van Zelst, Julia Maia

Writing – original draft: Iris van Zelst

Writing – review & editing: Iris van Zelst, Julia Maia, Ana-Catalina Plesa, Richard Ghail, Moritz Spühler

Data availability statement

The Jupyter Notebooks used to make the results and plot the figures as well as the CMT database and geospatial vector data (shapefiles) of the tectonic setting areas on Earth can be found in Van Zelst et al. (2024). Explanations of individual files in this repository and additional figures and tables are provided in the Supplementary Material. The Venus mapping data used here from Price and Suppe (1995); Price et al. (1996) can be found in the ArcGIS repository 'Venus Geology and Tectonics' at <https://www.arcgis.com/home/item.html?id=962dcfd6b5b64b21a922bc9b6c94ad78>. The topography maps were created using the VenusTopo719 data set (Wieczorek, 2015) and the radar image mosaics can be found in Pettengill (1992). Figures were made with Python in Jupyter Notebooks and Adobe Illustrator. We used the colourblind-friendly colour map from the IBM Design Library (David Nichols, 2022; retrieved: February 16, 2023).

References

- Abdrakhimov, A., & Basilevsky, A. (2002). Geology of the Venera and Vega landing-site regions. *Solar System Research*, *36*, 136–159.
- Aderhold, K., & Abercrombie, R. E. (2016). Seismotectonics of a diffuse plate boundary: Observations off the sumatra-andaman trench. *Journal of Geophysical Research: Solid Earth*, *121*(5), 3462–3478.
- Ágústsson, K., & Flóvenz, Ó. G. (2005). The thickness of the seismogenic crust in iceland and its implications for geothermal systems. In *Proceedings of the*

- 825 *world geothermal congress* (pp. 24–29).
- 826 Anderson, F. S., & Smrekar, S. E. (2006). Global mapping of crustal and litho-
827 spheric thickness on Venus. *Journal of Geophysical Research: Planets (1991–*
828 *2012)*, *111*(E8).
- 829 Angiboust, S., Wolf, S., Burov, E., Agard, P., & Yamato, P. (2012). Effect of fluid
830 circulation on subduction interface tectonic processes: Insights from thermo-
831 mechanical numerical modelling. *Earth and Planetary Science Letters*, *357*,
832 238–248.
- 833 Baes, M., Stern, R. J., Whattam, S., Gerya, T. V., & Sobolev, S. V. (2021). Plume-
834 induced subduction initiation: Revisiting models and observations. *Frontiers in*
835 *Earth Science*, *9*, 766604.
- 836 Banerdt, W. B., Smrekar, S. E., Banfield, D., Giardini, D., Golombek, M., Johnson,
837 C. L., ... others (2020). Initial results from the InSight mission on Mars.
838 *Nature Geoscience*, *13*(3), 183–189.
- 839 Basilevsky, A. T., & Head, J. W. (1997). Onset time and duration of corona activity
840 on venus: stratigraphy and history from photogeologic study of stereo images.
841 *Earth, Moon, and Planets*, *76*(1), 67–115.
- 842 Basilevsky, A. T., & McGill, G. E. (2007). Surface evolution of Venus. *Exploring*
843 *Venus as a terrestrial planet*, *176*, 23–43. doi: 10.1029/176GM04
- 844 Beroza, G., & Kanamori, H. (2015). 4.01 - Earthquake Seismology: An Introduction
845 and Overview. In G. Schubert (Ed.), *Treatise on geophysics* (Second ed., p. 1 -
846 50). Oxford: Elsevier.
- 847 Bjornnes, E., Johnson, B., & Evans, A. (2021). Estimating Venusian thermal condi-
848 tions using multiring basin morphology. *Nature Astronomy*, *5*(5), 498–502.
- 849 Boettcher, M. S., Hirth, G., & Evans, B. (2007). Olivine friction at the base of
850 oceanic seismogenic zones. *Journal of Geophysical Research: Solid Earth*,
851 *112*(B1).
- 852 Boneh, Y., Schottenfels, E., Kwong, K., Van Zelst, I., Tong, X., Eimer, M., ...
853 Zhan, Z. (2019). Intermediate-depth earthquakes controlled by incoming plate
854 hydration along bending-related faults. *Geophysical Research Letters*, *46*(7),
855 3688–3697. Retrieved from [https://agupubs.onlinelibrary.wiley.com/](https://agupubs.onlinelibrary.wiley.com/doi/abs/10.1029/2018GL081585)
856 [doi/abs/10.1029/2018GL081585](https://agupubs.onlinelibrary.wiley.com/doi/abs/10.1029/2018GL081585) doi: 10.1029/2018GL081585
- 857 Borrelli, M. E., O'Rourke, J. G., Smrekar, S. E., & Ostberg, C. M. (2021). A Global
858 Survey of Lithospheric Flexure at Steep-Sided Domical Volcanoes on Venus
859 Reveals Intermediate Elastic Thicknesses. *Journal of Geophysical Research:*
860 *Planets*, *126*(7), e2020JE006756.
- 861 Brissaud, Q., Krishnamoorthy, S., Jackson, J. M., Bowman, D. C., Komjathy, A.,
862 Cutts, J. A., ... Walsh, G. J. (2021). The first detection of an earthquake
863 from a balloon using its acoustic signature. *Geophysical Research Letters*,
864 *48*(12), e2021GL093013.
- 865 Brossier, J., Gilmore, M. S., & Head, J. W. (2022). Extended Rift-Associated Vol-
866 canism in Ganis Chasma, Venus Detected From Magellan Radar Emissivity.
867 *Geophysical Research Letters*, *49*(15), e2022GL099765.
- 868 Bulmer, M., & Guest, J. (1996). Modified volcanic domes and associated debris
869 aprons on Venus. *Geological Society, London, Special Publications*, *110*(1),
870 349–371.
- 871 Bulmer, M., Petley, D., Murphy, W., & Mantovani, F. (2006). Detecting slope de-
872 formation using two-pass differential interferometry: Implications for landslide
873 studies on Earth and other planetary bodies. *Journal of Geophysical Research:*
874 *Planets*, *111*(E6).
- 875 Bulmer, M. H. K. (2012). Landslides on other planets. In J. J. Clague & D. Stead
876 (Eds.), *Landslides: Types, mechanisms and modeling* (p. 393–408). Cambridge
877 University Press. doi: 10.1017/CBO9780511740367.033
- 878 Byrne, P. K., Ghail, R. C., Şengör, A. C., James, P. B., Klimczak, C., & Solomon,
879 S. C. (2021). A globally fragmented and mobile lithosphere on Venus. *Proceed-*

- 880 *ings of the National Academy of Sciences*, 118(26).
- 881 Byrne, P. K., & Krishnamoorthy, S. (2022). Estimates on the frequency of vol-
 882 canic eruptions on Venus. *Journal of Geophysical Research: Planets*, 127(1),
 883 e2021JE007040. doi: 10.1029/2021JE007040
- 884 Chen, W.-P., & Molnar, P. (1983). Focal depths of intracontinental and intraplate
 885 earthquakes and their implications for the thermal and mechanical properties
 886 of the lithosphere. *Journal of Geophysical Research: Solid Earth*, 88(B5),
 887 4183–4214.
- 888 Davaille, A., Smrekar, S. E., & Tomlinson, S. (2017). Experimental and observa-
 889 tional evidence for plume-induced subduction on Venus. *Nature Geoscience*,
 890 10(5), 349–355.
- 891 David Nichols. (2022; retrieved: February 16, 2023). *Coloring for Colorblindness*.
 892 (<http://tsitsul.in/blog/coloropt/>)
- 893 Dombard, A. J., Johnson, C. L., Richards, M. A., & Solomon, S. C. (2007). A mag-
 894 matic loading model for coronae on Venus. *Journal of Geophysical Research:*
 895 *Planets*, 112(E4).
- 896 Dragonì, M., & Piombo, A. (2003). A model for the formation of wrinkle ridges in
 897 volcanic plains on venus. *Physics of the Earth and Planetary Interiors*, 135(2-
 898 3), 161–171.
- 899 Dyar, M. D., Helbert, J., Cooper, R. F., Sklute, E. C., Maturilli, A., Mueller, N. T.,
 900 ... Smrekar, S. E. (2021). Surface weathering on Venus: Constraints from
 901 kinetic, spectroscopic, and geochemical data. *Icarus*, 358, 114139.
- 902 Dzierwonski, A. M., Chou, T.-A., & Woodhouse, J. H. (1981). Determination of
 903 earthquake source parameters from waveform data for studies of global and
 904 regional seismicity. *Journal of Geophysical Research: Solid Earth*, 86(B4),
 905 2825–2852.
- 906 Ekström, G., Nettles, M., & Dziewoński, A. (2012). The global CMT project 2004–
 907 2010: Centroid-moment tensors for 13,017 earthquakes. *Physics of the Earth*
 908 *and Planetary Interiors*, 200, 1–9.
- 909 Emmerson, B., & McKenzie, D. (2007). Thermal structure and seismicity of sub-
 910 ducting lithosphere. *Physics of the Earth and Planetary Interiors*, 163(1-4),
 911 191–208.
- 912 Filiberto, J., Trang, D., Treiman, A. H., & Gilmore, M. S. (2020). Present-day
 913 volcanism on Venus as evidenced from weathering rates of olivine. *Science Ad-*
 914 *vances*, 6(1), eaax7445.
- 915 Foley, B. J., Bercovici, D., & Landuyt, W. (2012). The conditions for plate tecton-
 916 ics on super-earths: inferences from convection models with damage. *Earth and*
 917 *Planetary Science Letters*, 331, 281–290.
- 918 Foster, A., & Nimmo, F. (1996). Comparisons between the rift systems of East
 919 Africa, Earth and Beta Regio, Venus. *Earth and Planetary Science Letters*,
 920 143(1-4), 183–195. doi: 10.1016/0012-821X(96)00146-X
- 921 Frank, S. L., & Head, J. W. (1990). Ridge belts on venus: Morphology and origin.
 922 *Earth, Moon, and Planets*, 50, 421–470.
- 923 Ganesh, I., Herrick, R. R., & Kremic, T. (2023). Bounds on Venus’s seismicity from
 924 theoretical and analog estimations. In *LPSC Abstracts, No. 2806*.
- 925 Garcia, R. F., Klotz, A., Hertzog, A., Martin, R., G erier, S., Kassarian, E., ...
 926 Mimoun, D. (2022). Infrasound from large earthquakes recorded on a net-
 927 work of balloons in the stratosphere. *Geophysical Research Letters*, 49(15),
 928 e2022GL098844.
- 929 Garcia, R. F., van Zelst, I., Kawamura, T., N asholm, S. P., Horleston, A. C.,
 930 Klaasen, S., ... others (2024). Seismic wave detectability on Venus using
 931 ground deformation sensors, infrasound sensors on balloons and airglow im-
 932 agers. *Authorea Preprints*.
- 933 Gerya, T. V. (2014). Plume-induced crustal convection: 3d thermomechanical model
 934 and implications for the origin of novae and coronae on venus. *Earth and Plan-*

- etary *Science Letters*, *391*, 183–192.
- 935 Ghail, R., Wilson, C. F., & Widemann, T. (2016). EnVision M5 Venus or-
 936 biter proposal: Opportunities and challenges. In *Aas/division for plane-*
 937 *tary sciences meeting abstracts# 48* (Vol. 48, pp. 216–08). doi: [https://](https://ui.adsabs.harvard.edu/abs/2016DPS....4821608G)
 938 ui.adsabs.harvard.edu/abs/2016DPS....4821608G
- 939 Giardini, D., Lognonné, P., Banerdt, W. B., Pike, W. T., Christensen, U., Ceylan,
 940 S., . . . others (2020). The seismicity of Mars. *Nature Geoscience*, *13*(3),
 941 205–212.
- 942 Gillmann, C., Way, M. J., Avice, G., Breuer, D., Golabek, G. J., Höning, D., . . .
 943 others (2022). The long-term evolution of the atmosphere of venus: Processes
 944 and feedback mechanisms: Interior-exterior exchanges. *Space Science Reviews*,
 945 *218*(7), 56.
- 946 Gilmore, M., Mueller, N., & Helbert, J. (2015). VIRTIS emissivity of Alpha Re-
 947 gio, Venus, with implications for tessera composition. *Icarus*, *254*, 350–361.
 948 Retrieved from <https://doi.org/10.1016/j.icarus.2015.04.008> doi:
 949 10.1016/j.icarus.2015.04.008
- 950 Gilmore, M. S., Darby Dyar, M., Mueller, N., Brossier, J., Santos, A. R., Ivanov,
 951 M., . . . Helbert, J. (2023). Mineralogy of the Venus surface. *Space Science*
 952 *Reviews*, *219*(7), 52.
- 953 Golombek, M. P., Banerdt, W. B., Tanaka, K. L., & Tralli, D. M. (1992). A predic-
 954 tion of mars seismicity from surface faulting. *Science*, *258*(5084), 979–981.
- 955 Graff, J., Ernst, R. E., & Samson, C. (2018). Evidence for triple-junction rifting
 956 focussed on local magmatic centres along Parga Chasma, Venus. *Icarus*, *306*,
 957 122–138.
- 958 Green, H. W., & Houston, H. (1995). The mechanics of deep earthquakes. *Annual*
 959 *Review of Earth and Planetary Sciences*, *23*(1), 169–213.
- 960 Grimm, R., & Hess, P. (1997). The crust of venus. *Venus II: Geology, geophysics, at-*
 961 *mosphere, and solar wind environment*, 1205.
- 962 Grimm, R. E. (1994). Recent deformation rates on venus. *Journal of Geophysical*
 963 *Research: Planets*, *99*(E11), 23163–23171.
- 964 Grindrod, P. M., & Hoogenboom, T. (2006). Venus: the corona conundrum. *Astron-*
 965 *omy & Geophysics*, *47*(3), 3–16.
- 966 Grinspoon, D. H. (1993). Implications of the high d/h ratio for the sources of water
 967 in venus’ atmosphere. *Nature*, *363*(6428), 428–431.
- 968 Gülcher, A. J., Gerya, T. V., Montési, L. G., & Munch, J. (2020). Corona struc-
 969 tures driven by plume–lithosphere interactions and evidence for ongoing plume
 970 activity on Venus. *Nature Geoscience*, *13*(8), 547–554.
- 971 Gülcher, A. J., Yu, T.-Y., & Gerya, T. V. (2023). Tectono-Magmatic Evolution of
 972 Asymmetric Coronae on Venus: Topographic Classification and 3D Thermo-
 973 Mechanical Modeling. *Journal of Geophysical Research: Planets*, *128*(11),
 974 e2023JE007978.
- 975 Gutenberg, B., & Richter, C. F. (1956). Magnitude and energy of earthquakes. *An-*
 976 *nals of Geophysics*, *9*(1), 1–15.
- 977 Gutscher, M.-A., & Peacock, S. M. (2003). Thermal models of flat subduction and
 978 the rupture zone of great subduction earthquakes. *Journal of Geophysical Re-*
 979 *search: Solid Earth*, *108*(B1), ESE–2.
- 980 Hacker, B. R., Peacock, S. M., Abers, G. A., & Holloway, S. D. (2003). Subduction
 981 factory 2. Are intermediate-depth earthquakes in subducting slabs linked to
 982 metamorphic dehydration reactions? *Journal of Geophysical Research: Solid*
 983 *Earth*, *108*(B1).
- 984 Hahn, R. M., & Byrne, P. K. (2023). A morphological and spatial analysis of
 985 volcanoes on Venus. *Journal of Geophysical Research: Planets*, *128*(4),
 986 e2023JE007753. doi: 10.1029/2023JE007753
- 987 Harris, L. B., & Bédard, J. H. (2015). Interactions between continent-like ‘drift’,
 988 rifting and mantle flow on venus: gravity interpretations and earth analogues.
- 989

- 990 *Geological Society, London, Special Publications, 401*(1), 327–356.
- 991 Hasterok, D., Halpin, J. A., Collins, A. S., Hand, M., Kreemer, C., Gard, M. G., &
992 Glorie, S. (2022). New maps of global geological provinces and tectonic plates.
993 *Earth-Science Reviews, 231*, 104069.
- 994 He, C., Wang, Z., & Yao, W. (2007). Frictional sliding of gabbro gouge under hy-
995 drothermal conditions. *Tectonophysics, 445*(3-4), 353–362.
- 996 Head, J. W. (1990). Venus trough-and-ridge tessera: Analog to Earth oceanic crust
997 formed at spreading centers? *Journal of Geophysical Research: Solid Earth,*
998 *95*(B5), 7119–7132.
- 999 Herrick, R. R. (1999). Small mantle upwellings are pervasive on venus and earth.
1000 *Geophysical research letters, 26*(6), 803–806.
- 1001 Herrick, R. R., Bjonnes, E. T., Carter, L. M., Gerya, T., Ghail, R. C., Gillmann, C.,
1002 ... others (2023). Resurfacing history and volcanic activity of venus. *Space*
1003 *Science Reviews, 219*(4), 29.
- 1004 Herrick, R. R., & Hensley, S. (2023). Surface changes observed on a Venusian vol-
1005 cano during the Magellan mission. *Science, 379*(6638), 1205–1208. doi: 10
1006 .1126/science.abm7735
- 1007 Hoogenboom, T., & Houseman, G. A. (2006). Rayleigh–Taylor instability as a mech-
1008 anism for corona formation on Venus. *Icarus, 180*(2), 292–307.
- 1009 Houston, H. (2015). 4.13 - Deep Earthquakes. In G. Schubert (Ed.), *Treatise on geo-*
1010 *physics* (Second ed., p. 329 - 354). Oxford: Elsevier. Retrieved from [http://](http://www.sciencedirect.com/science/article/pii/B9780444538024000798)
1011 www.sciencedirect.com/science/article/pii/B9780444538024000798
1012 doi: <https://doi.org/10.1016/B978-0-444-53802-4.00079-8>
- 1013 Hyndman, R. D., & Wang, K. (1993). Thermal constraints on the zone of major
1014 thrust earthquake failure: The cascadia subduction zone. *Journal of Geophysi-*
1015 *cal Research: Solid Earth, 98*(B2), 2039–2060.
- 1016 Hyndman, R. D., Yamano, M., & Oleskevich, D. A. (1997). The seismogenic zone of
1017 subduction thrust faults. *Island Arc, 6*(3), 244–260.
- 1018 Ivanov, M. A., & Head, J. W. (2011). Global geological map of Venus. *Planetary*
1019 *and Space Science, 59*(13), 1559–1600.
- 1020 James, P. B., Zuber, M. T., & Phillips, R. J. (2013). Crustal thickness and support
1021 of topography on Venus. *Journal of Geophysical Research: Planets, 118*(4),
1022 859–875.
- 1023 Janes, D. M., Squyres, S. W., Bindschadler, D. L., Baer, G., Schubert, G., Sharp-
1024 ton, V. L., & Stofan, E. R. (1992). Geophysical models for the formation
1025 and evolution of coronae on Venus. *Journal of Geophysical Research: Planets,*
1026 *97*(E10), 16055–16067.
- 1027 Johnson, C. L., & Richards, M. A. (2003). A conceptual model for the relationship
1028 between coronae and large-scale mantle dynamics on venus. *Journal of Geo-*
1029 *physical Research: Planets, 108*(E6).
- 1030 Jull, M. G., & Arkani-Hamed, J. (1995). The implications of basalt in the formation
1031 and evolution of mountains on venus. *Physics of the Earth and Planetary Inte-*
1032 *riors, 89*(3-4), 163–175.
- 1033 Jung, H., Green Ii, H. W., & Dobrzhinetskaya, L. F. (2004). Intermediate-depth
1034 earthquake faulting by dehydration embrittlement with negative volume
1035 change. *Nature, 428*(6982), 545–549.
- 1036 Jurdy, D. M., & Stoddard, P. R. (2007, 01). The coronae of Venus: Impact, plume,
1037 or other origin? In *Plates, Plumes and Planetary Processes*. Geological Society
1038 of America. doi: 10.1130/2007.2430(40)
- 1039 Karato, S.-i., & Barbot, S. (2018). Dynamics of fault motion and the origin of con-
1040 trasting tectonic style between Earth and Venus. *Scientific Reports, 8*(1), 1–
1041 11.
- 1042 Kelemen, P. B., & Hirth, G. (2007). A periodic shear-heating mechanism for
1043 intermediate-depth earthquakes in the mantle. *Nature, 446*(7137), 787–790.
- 1044 Kiefer, W. S., & Peterson, K. (2003). Mantle and crustal structure in phoebe

- 1045 regio and devana chasma, venus. *Geophysical Research Letters*, 30(1), 5-1-5-
 1046 4. Retrieved from [https://agupubs.onlinelibrary.wiley.com/doi/abs/](https://agupubs.onlinelibrary.wiley.com/doi/abs/10.1029/2002GL015762)
 1047 [10.1029/2002GL015762](https://agupubs.onlinelibrary.wiley.com/doi/abs/10.1029/2002GL015762)
- 1048 Kiefer, W. S., & Swafford, L. C. (2006). Topographic analysis of Devana Chasma,
 1049 Venus: Implications for rift system segmentation and propagation. *Journal of*
 1050 *structural geology*, 28(12), 2144–2155.
- 1051 Knapmeyer, M., Oberst, J., Hauber, E., Wählisch, M., Deuchler, C., & Wagner, R.
 1052 (2006). Working models for spatial distribution and level of mars’ seismicity.
 1053 *Journal of Geophysical Research: Planets*, 111(E11).
- 1054 Koch, D. M., & Manga, M. (1996). Neutrally buoyant diapirs: A model for venus
 1055 coronae. *Geophysical Research Letters*, 23(3), 225–228.
- 1056 Kremic, T., Ghail, R., Gilmore, M., Hunter, G., Kiefer, W., Limaye, S., ... Wilson,
 1057 C. (2020). Long-duration Venus lander for seismic and atmospheric science.
 1058 *Planetary and space science*, 190, 104961. doi: [https://doi.org/10.1016/](https://doi.org/10.1016/j.pss.2020.104961)
 1059 [j.pss.2020.104961](https://doi.org/10.1016/j.pss.2020.104961)
- 1060 Krishnamoorthy, S., & Bowman, D. C. (2023). A “Floatilla” of Airborne Seismome-
 1061 ters for Venus. *Geophysical Research Letters*, 50(2), e2022GL100978.
- 1062 Krishnamoorthy, S., Komjathy, A., Cutts, J. A., Lognonne, P., Garcia, R. F., Pan-
 1063 ning, M. P., ... others (2020). *Seismology on Venus with infrasound obser-*
 1064 *ventions from balloon and orbit* (Tech. Rep.). Sandia National Lab.(SNL-NM),
 1065 Albuquerque, NM (United States).
- 1066 Ksanfomaliti, L., Zubkova, V., Morozov, N., & Petrova, E. (1982). Microseisms at
 1067 the VENERA-13 and VENERA-14 Landing Sites. *Soviet Astronomy Letters*,
 1068 8, 241.
- 1069 Le Feuvre, M., & Wieczorek, M. A. (2011). Nonuniform cratering of the Moon
 1070 and a revised crater chronology of the inner Solar System. *Icarus*, 214(1), 1–
 1071 20. Retrieved from <https://doi.org/10.1016/j.icarus.2011.03.010> doi:
 1072 [10.1016/j.icarus.2011.03.010](https://doi.org/10.1016/j.icarus.2011.03.010)
- 1073 Lenardic, A., Jellinek, A., & Moresi, L.-N. (2008). A climate induced transition in
 1074 the tectonic style of a terrestrial planet. *Earth and Planetary Science Letters*,
 1075 271(1-4), 34–42.
- 1076 Lognonné, P., & Johnson, C. (2015). 10.03—planetary seismology. *Treatise on geo-*
 1077 *physics*, 2, 65–120.
- 1078 Lorenz, R. D. (2012). Planetary seismology—Expectations for lander and wind noise
 1079 with application to Venus. *Planetary and Space Science*, 62(1), 86–96.
- 1080 Lourenço, D. L., Rozel, A. B., Ballmer, M. D., & Tackley, P. J. (2020). Plutonic-
 1081 squishy lid: a new global tectonic regime generated by intrusive magma-
 1082 tism on Earth-like planets. *Geochemistry, Geophysics, Geosystems*, 21(4),
 1083 e2019GC008756.
- 1084 Mackwell, S., Zimmerman, M., & Kohlstedt, D. (1998). High-temperature deformation
 1085 of dry diabase with application to tectonics on venus. *Journal of Geophys-*
 1086 *ical Research: Solid Earth*, 103(B1), 975–984.
- 1087 Maia, J. S., & Wieczorek, M. A. (2022). Lithospheric Structure of Venusian Crustal
 1088 Plateaus. *Journal of Geophysical Research: Planets*, e2021JE007004.
- 1089 Maia, J. S., Wieczorek, M. A., & Plesa, A. (2023). The Mantle Viscosity Structure
 1090 of Venus. *Geophysical Research Letters*, 50(15). Retrieved from [http://dx](http://dx.doi.org/10.1029/2023GL103847)
 1091 [.doi.org/10.1029/2023GL103847](http://dx.doi.org/10.1029/2023GL103847) doi: [10.1029/2023gl103847](https://doi.org/10.1029/2023gl103847)
- 1092 Marcq, E., Bertaux, J.-L., Montmessin, F., & Belyaev, D. (2013). Variations of
 1093 sulphur dioxide at the cloud top of Venus’s dynamic atmosphere. *Nature geo-*
 1094 *science*, 6(1), 25–28. doi: <https://doi.org/10.1038/ngeo1650>
- 1095 McGill, G. E., Steenstrup, S. J., Barton, C., & Ford, P. G. (1981). Continental
 1096 rifting and the origin of beta regio, venus. *Geophysical Research Letters*, 8(7),
 1097 737–740.
- 1098 McKenzie, D., Jackson, J., & Priestley, K. (2005). Thermal structure of oceanic and
 1099 continental lithosphere. *Earth and Planetary Science Letters*, 233(3-4), 337–

- 1100 349.
- 1101 McKinnon, W. B., Zahnle, K. J., Ivanov, B. A., & Melosh, H. (1997). Cratering on
1102 Venus: Models and observations. *Venus II: Geology, geophysics, atmosphere,
1103 and solar wind environment*, 969.
- 1104 Melgar, D., Ruiz-Angulo, A., Garcia, E. S., Manea, M., Manea, V. C., Xu, X., ...
1105 others (2018). Deep embrittlement and complete rupture of the lithosphere
1106 during the m w 8.2 tehuantepec earthquake. *Nature Geoscience*, 11(12),
1107 955–960.
- 1108 Molnar, P. (2020). The brittle-plastic transition, earthquakes, temperatures,
1109 and strain rates. *Journal of Geophysical Research: Solid Earth*, 125(7),
1110 e2019JB019335.
- 1111 Musser Jr, G. S., & Squyres, S. W. (1997). A coupled thermal-mechanical model
1112 for corona formation on venus. *Journal of Geophysical Research: Planets*,
1113 102(E3), 6581–6595.
- 1114 Nakamura, Y., Latham, G. V., & Dorman, H. J. (1982). Apollo lunar seismic experi-
1115 ment—Final summary. *Journal of Geophysical Research: Solid Earth*, 87(S01),
1116 A117–A123.
- 1117 Namiki, N., & Solomon, S. C. (1998). Volcanic degassing of argon and helium and
1118 the history of crustal production on venus. *Journal of Geophysical Research:
1119 Planets*, 103(E2), 3655–3677.
- 1120 Oberst, J. (1987). Unusually high stress drops associated with shallow moonquakes.
1121 *Journal of Geophysical Research: Solid Earth*, 92(B2), 1397–1405.
- 1122 O’Rourke, J., Wilson, C., Borrelli, M., Byrne, P. K., Dumoulin, C., Ghail, R., ...
1123 Westall, F. (2023). Venus, the Planet: Introduction to the Evolution of Earth’s
1124 Sister Planet. *Space Science Reviews*, 219(10).
- 1125 Pavri, B., Head III, J. W., Klose, K. B., & Wilson, L. (1992). Steep-sided domes on
1126 Venus: Characteristics, geologic setting, and eruption conditions from Magellan
1127 data. *Journal of Geophysical Research: Planets*, 97(E8), 13445–13478.
- 1128 Peacock, S. M. (2001). Are the lower planes of double seismic zones caused by ser-
1129 pentine dehydration in subducting oceanic mantle? *Geology*, 29(4), 299–302.
- 1130 Peacock, S. M., & Hyndman, R. D. (1999). Hydrous minerals in the mantle wedge
1131 and the maximum depth of subduction thrust earthquakes. *Geophysical Re-
1132 search Letters*, 26(16), 2517–2520.
- 1133 Pettengill, G. (1992). *MGN V RADAR SYSTEM DERIVED MIDR COM-
1134 PRESSED THRICE V1.0*. NASA Planetary Data System. Retrieved from
1135 [https://pds.nasa.gov/ds-view/pds/viewProfile.jsp?dsid=MGN-V-RDRS-5-
1136 -MIDR-C3-V1.0](https://pds.nasa.gov/ds-view/pds/viewProfile.jsp?dsid=MGN-V-RDRS-5-MIDR-C3-V1.0)
- 1137 Phillips, R. J., Kaula, W. M., McGill, G. E., & Malin, M. C. (1981). Tectonics and
1138 evolution of venus. *Science*, 212(4497), 879–887.
- 1139 Phillips, R. J., & Malin, M. C. (1984). Tectonics of venus. *Annual Review of Earth
1140 and Planetary Sciences*, 12(1), 411–443.
- 1141 Piskorz, D., Elkins-Tanton, L. T., & Smrekar, S. E. (2014). Coronae formation
1142 on venus via extension and lithospheric instability. *Journal of Geophysical Re-
1143 search: Planets*, 119(12), 2568–2582.
- 1144 Price, M., & Suppe, J. (1995). Constraints on the resurfacing history of Venus from
1145 the hypsometry and distribution of volcanism, tectonism, and impact craters.
1146 *Earth, Moon, and Planets*, 71(1-2), 99–145.
- 1147 Price, M., Watson, G., Suppe, J., & Brankman, C. (1996). Dating volcanism and
1148 rifting on Venus using impact crater densities. *Journal of Geophysical Re-
1149 search: Planets*, 101(E2), 4657–4671.
- 1150 Prieto, G. A., Froment, B., Yu, C., Poli, P., & Abercrombie, R. (2017). Earthquake
1151 rupture below the brittle-ductile transition in continental lithospheric mantle.
1152 *Science Advances*, 3(3), e1602642.
- 1153 Regorda, A., Thieulot, C., Van Zelst, I., Erdős, Z., Maia, J., & Buiters, S. (2023).
1154 Rifting Venus: insights from numerical modeling. *Journal of Geophysical*

- 1155 *Research: Planets*, 128(3), e2022JE007588. doi: 10.1029/2022JE007588
- 1156 Richards, F., Hoggard, M., Cowton, L., & White, N. (2018). Reassessing the thermal
1157 structure of oceanic lithosphere with revised global inventories of basement
1158 depths and heat flow measurements. *Journal of Geophysical Research: Solid
1159 Earth*, 123(10), 9136–9161.
- 1160 Rolf, T., Weller, M., Gülcher, A., Byrne, P., O’Rourke, J. G., Herrick, R., . . . others
1161 (2022). Dynamics and evolution of Venus’ mantle through time. *Space Science
1162 Reviews*, 218(8), 70.
- 1163 Romeo, I., & Turcotte, D. (2008). Pulsating continents on Venus: An explanation
1164 for crustal plateaus and tessera terrains. *Earth and Planetary Science Letters*,
1165 276(1-2), 85–97. Retrieved from [https://doi.org/10.1016/j.epsl.2008.09](https://doi.org/10.1016/j.epsl.2008.09.009)
1166 .009 doi: 10.1016/j.epsl.2008.09.009
- 1167 Sabbeth, L., Carrington, M. A., & Smrekar, S. E. (2024). Constraints on corona
1168 formation from an analysis of topographic rims and fracture annuli. *Earth and
1169 Planetary Science Letters*, 633, 118568.
- 1170 Sabbeth, L., Smrekar, S., & Stock, J. (2023a). Estimated seismicity of Venusian
1171 wrinkle ridges based on fault scaling relationships. *Earth and Planetary Sci-
1172 ence Letters*, 619, 118308. Retrieved from [https://www.sciencedirect.com/
1173 science/article/pii/S0012821X23003217](https://www.sciencedirect.com/science/article/pii/S0012821X23003217) doi: 10.1016/j.epsl.2023.118308
- 1174 Sabbeth, L., Smrekar, S. E., & Stock, J. M. (2023b). Using InSight data to calibrate
1175 seismicity from remote observations of surface faulting. *Journal of Geophysical
1176 Research: Planets*, 128(6), e2022JE007686. Retrieved from [https://agupubs
1177 .onlinelibrary.wiley.com/doi/abs/10.1029/2022JE007686](https://agupubs.onlinelibrary.wiley.com/doi/abs/10.1029/2022JE007686) doi: 10.1029/
1178 2022JE007686
- 1179 Salvador, A., Avice, G., Breuer, D., Gillmann, C., Jacobson, S., Lammer, H., . . .
1180 others (2022). Magma ocean, water, and the early atmosphere of venus. *Space
1181 Sci Rev.*
- 1182 Scholz, C. H. (2019). *The mechanics of earthquakes and faulting*. Cambridge univer-
1183 sity press.
- 1184 Schools, J., & Smrekar, S. E. (2024). Formation of coronae topography and frac-
1185 tures via plume buoyancy and melting. *Earth and Planetary Science Letters*,
1186 633, 118643.
- 1187 Schubert, G., & Sandwell, D. (1995). A global survey of possible subduction sites on
1188 venus. *Icarus*, 117(1), 173–196.
- 1189 Seno, T. (2009). Determination of the pore fluid pressure ratio at seismogenic
1190 megathrusts in subduction zones: Implications for strength of asperities and
1191 Andean-type mountain building. *Journal of Geophysical Research: Solid Earth*,
1192 114(B5).
- 1193 Seton, M., Müller, R. D., Zahirovic, S., Williams, S., Wright, N. M., Cannon, J., . . .
1194 McGirr, R. (2020). A global data set of present-day oceanic crustal age and
1195 seafloor spreading parameters. *Geochemistry, Geophysics, Geosystems*, 21(10),
1196 e2020GC009214.
- 1197 Smrekar, S. E., Davaille, A., & Sotin, C. (2018). Venus interior structure and dy-
1198 namics. *Space Science Reviews*, 214(5), 1–34.
- 1199 Smrekar, S. E., Dyar, D., Helbert, J., Hensley, S., Nunes, D., & Whitten, J. (2020).
1200 VERITAS (Venus Emissivity, Radio Science, InSAR, Topography, and Spec-
1201 troscopy): A proposed Discovery mission. In *European planetary science
1202 congress* (p. EPSC2020-447). doi: <https://doi.org/10.5194/eps2020-447>
- 1203 Smrekar, S. E., Ostberg, C., & O’Rourke, J. G. (2023). Earth-like lithospheric thick-
1204 ness and heat flow on Venus consistent with active rifting. *Nature Geoscience*,
1205 16(1), 13–18.
- 1206 Smrekar, S. E., & Sotin, C. (2012). Constraints on mantle plumes on venus: Implica-
1207 tions for volatile history. *Icarus*, 217(2), 510–523.
- 1208 Smrekar, S. E., & Stofan, E. R. (1997). Corona formation and heat loss on venus by
1209 coupled upwelling and delamination. *Science*, 277(5330), 1289–1294.

- 1210 Smrekar, S. E., & Stofan, E. R. (1999). Origin of corona-dominated topographic
1211 rises on Venus. *Icarus*, *139*(1), 100–115.
- 1212 Smrekar, S. E., Stofan, E. R., Mueller, N., Treiman, A., Elkins-Tanton, L., Helbert,
1213 J., ... Drossart, P. (2010). Recent hotspot volcanism on Venus from VIRTIS
1214 emissivity data. *Science*, *328*(5978), 605–608. doi: [https://doi.org/10.1126/
1215 science.1186785](https://doi.org/10.1126/science.1186785)
- 1216 Solomon, S. (1993). The geophysics of Venus. *Physics Today*, *46*(7), 48–55.
- 1217 Solomon, S. C., Bullock, M. A., & Grinspoon, D. H. (1999). Climate change as a
1218 regulator of tectonics on Venus. *Science*, *286*(5437), 87–90.
- 1219 Solomon, S. C., Head, J. W., Kaula, W. M., McKenzie, D., Parsons, B., Phillips,
1220 R. J., ... Talwani, M. (1991). Venus Tectonics: Initial Analysis from Magellan.
1221 *Science*, *252*(5003), 297–312. Retrieved from [https://www.science.org/doi/
1222 abs/10.1126/science.252.5003.297](https://www.science.org/doi/abs/10.1126/science.252.5003.297) doi: 10.1126/science.252.5003.297
- 1223 Spencer, J. E. (2001). Possible giant metamorphic core complex at the center of
1224 Artemis Corona, Venus. *Geological Society of America Bulletin*, *113*(3), 333–
1225 345.
- 1226 Squyres, S. W., Janes, D., Baer, G., Bindschadler, D. L., Schubert, G., Sharpton,
1227 V. L., & Stofan, E. R. (1992). The morphology and evolution of coronae on
1228 Venus. *Journal of Geophysical Research: Planets*, *97*(E8), 13611–13634.
- 1229 Stein, S., & Wysession, M. (2009). *An introduction to seismology, earthquakes, and
1230 earth structure*. John Wiley & Sons.
- 1231 Stevenson, D. J., Cutts, J. A., Mimoun, D., Arrowsmith, S., Banerdt, W. B., Blom,
1232 P., ... others (2015). Probing the interior structure of Venus.
- 1233 Stoddard, P. R., & Jurdy, D. M. (2012). Topographic comparisons of uplift fea-
1234 tures on Venus and Earth: Implications for Venus tectonics. *Icarus*, *217*(2),
1235 524–533.
- 1236 Stofan, E., Saunders, R., Senske, D., Nock, K., Tralli, D., Lundgren, P., ... others
1237 (1993). Venus interior structure mission (VISM): Establishing a seismic network
1238 on Venus. In *Advanced technologies for planetary instruments*.
- 1239 Stofan, E. R., Bindschadler, D. L., Head, J. W., & Parmentier, E. M. (1991).
1240 Corona structures on Venus: Models of origin. *Journal of Geophysical Re-
1241 search: Planets*, *96*(E4), 20933–20946.
- 1242 Stofan, E. R., Sharpton, V. L., Schubert, G., Baer, G., Bindschadler, D. L., Janes,
1243 D. M., & Squyres, S. W. (1992). Global distribution and characteristics of
1244 coronae and related features on Venus: Implications for origin and relation
1245 to mantle processes. *Journal of Geophysical Research: Planets (1991–2012)*,
1246 *97*(E8), 13347–13378.
- 1247 Stofan, E. R., Smrekar, S. E., Bindschadler, D. L., & Senske, D. A. (1995). Large
1248 topographic rises on Venus: Implications for mantle upwelling. *Journal of Geo-
1249 physical Research: Planets*, *100*(E11), 23317–23328. doi: 10.1029/95JE01834
- 1250 Strom, R. G., Schaber, G. G., & Dawson, D. D. (1994). The global resurfacing of
1251 Venus. *Journal of Geophysical Research: Planets (1991–2012)*, *99*(E5), 10899–
1252 10926.
- 1253 Sulcanese, D., Mitri, G., & Mastrogiuseppe, M. (2024). Evidence of ongoing volcanic
1254 activity on Venus revealed by Magellan radar. *Nature Astronomy*, 1–10.
- 1255 Tian, Y., Herrick, R. R., West, M. E., & Kremic, T. (2023). Mitigating Power and
1256 Memory Constraints on a Venusian Seismometer. *Seismological Society of
1257 America*, *94*(1), 159–171.
- 1258 Tichelaar, B. W., & Ruff, L. J. (1993). Depth of seismic coupling along subduction
1259 zones. *Journal of Geophysical Research: Solid Earth*, *98*(B2), 2017–2037.
- 1260 van Dinther, Y., Gerya, T. V., Dalguer, L. A., Corbi, F., Funicello, F., & Mai,
1261 P. M. (2013). The seismic cycle at subduction thrusts: 2. Dynamic implica-
1262 tions of geodynamic simulations validated with laboratory models. *Journal of
1263 Geophysical Research: Solid Earth*, *118*(4), 1502–1525.
- 1264 van Dinther, Y., Gerya, T. V., Dalguer, L. A., Mai, P. M., Morra, G., & Giardini,

- 1265 D. (2013). The seismic cycle at subduction thrusts: Insights from seismo-
 1266 thermo-mechanical models. *Journal of Geophysical Research: Solid Earth*,
 1267 *118*(12), 6183–6202.
- 1268 van Dinther, Y., Mai, P. M., Dalguer, L. A., & Gerya, T. V. (2014). Modeling the
 1269 seismic cycle in subduction zones: The role and spatiotemporal occurrence of
 1270 off-megathrust earthquakes. *Geophysical Research Letters*, *41*(4), 1194–1201.
- 1271 Van Zelst, I. (2022). Comment on “Estimates on the frequency of volcanic eruptions
 1272 on Venus” by Byrne & Krishnamoorthy (2022). *Journal of Geophysical
 1273 Research: Planets*, *127*(12), e2022JE007448. doi: 10.1029/2022JE007448
- 1274 Van Zelst, I., Maia, J., Plesa, A.-C., Ghail, R., & Spühler, M. (2024). *Data & scripts
 1275 - Estimates on the possible annual seismicity of Venus [Data set]*. Zenodo. doi:
 1276 10.5281/zenodo.10539251
- 1277 Van Zelst, I., Thieulot, C., & Craig, T. J. (2023). The effect of temperature-
 1278 dependent material properties on simple thermal models of subduction zones.
 1279 *Solid Earth*, *14*(7), 683–707. Retrieved from [https://se.copernicus.org/
 1280 articles/14/683/2023/](https://se.copernicus.org/articles/14/683/2023/) doi: 10.5194/se-14-683-2023
- 1281 Van Zelst, I., Wollherr, S., Gabriel, A.-A., Madden, E. H., & van Dinther, Y. (2019).
 1282 Modeling megathrust earthquakes across scales: one-way coupling from geo-
 1283 dynamics and seismic cycles to dynamic rupture. *Journal of Geophysical
 1284 Research: Solid Earth*, *124*(11), 11414–11446. doi: 10.1029/2019JB017539
- 1285 Wang, J., Zhao, D., & Yao, Z. (2017). Seismic anisotropy evidence for dehydration
 1286 embrittlement triggering intermediate-depth earthquakes. *Scientific reports*,
 1287 *7*(1), 1–9.
- 1288 Weller, M., Lenardic, A., & O’Neill, C. (2015). The effects of internal heating and
 1289 large scale climate variations on tectonic bi-stability in terrestrial planets.
 1290 *Earth and Planetary Science Letters*, *420*, 85–94.
- 1291 Widemann, T., Smrekar, S. E., Garvin, J. B., Straume-Lindner, A. G., Ocampo,
 1292 A. C., Schulte, M. D., ... others (2023). Venus evolution through time: key
 1293 science questions, selected mission concepts and future investigations. *Space
 1294 Science Reviews*, *219*(7), 56.
- 1295 Wieczorek, M. A. (2015). *Spherical harmonic model of the planet Venus:
 1296 VenusTopo719*. Zenodo. Retrieved from [https://zenodo.org/record/
 1297 3870926](https://zenodo.org/record/3870926)
- 1298 Williams, N. R., Bell III, J. F., Watters, T. R., Banks, M. E., Daud, K., & French,
 1299 R. A. (2019). Evidence for recent and ancient faulting at mare frigoris and
 1300 implications for lunar tectonic evolution. *Icarus*, *326*, 151–161.
- 1301 Wright, T. J., Elliott, J. R., Wang, H., & Ryder, I. (2013). Earthquake cycle deforma-
 1302 tion and the Moho: Implications for the rheology of continental lithosphere.
 1303 *Tectonophysics*, *609*, 504–523.
- 1304 Yamasaki, T., & Seno, T. (2003). Double seismic zone and dehydration embrit-
 1305 tlement of the subducting slab. *Journal of Geophysical Research: Solid Earth*,
 1306 *108*(B4).
- 1307 Zhong, S.-S., Zhao, Y.-Y. S., Lin, H., Chang, R., Qi, C., Wang, J., ... others (2023).
 1308 High-temperature oxidation of magnesium-and iron-rich olivine under a co2
 1309 atmosphere: Implications for venus. *Remote Sensing*, *15*(8), 1959.
- 1310 Zuber, M. (1990). Ridge belts: Evidence for regional-and local-scale deformation on
 1311 the surface of venus. *Geophysical Research Letters*, *17*(9), 1369–1372.

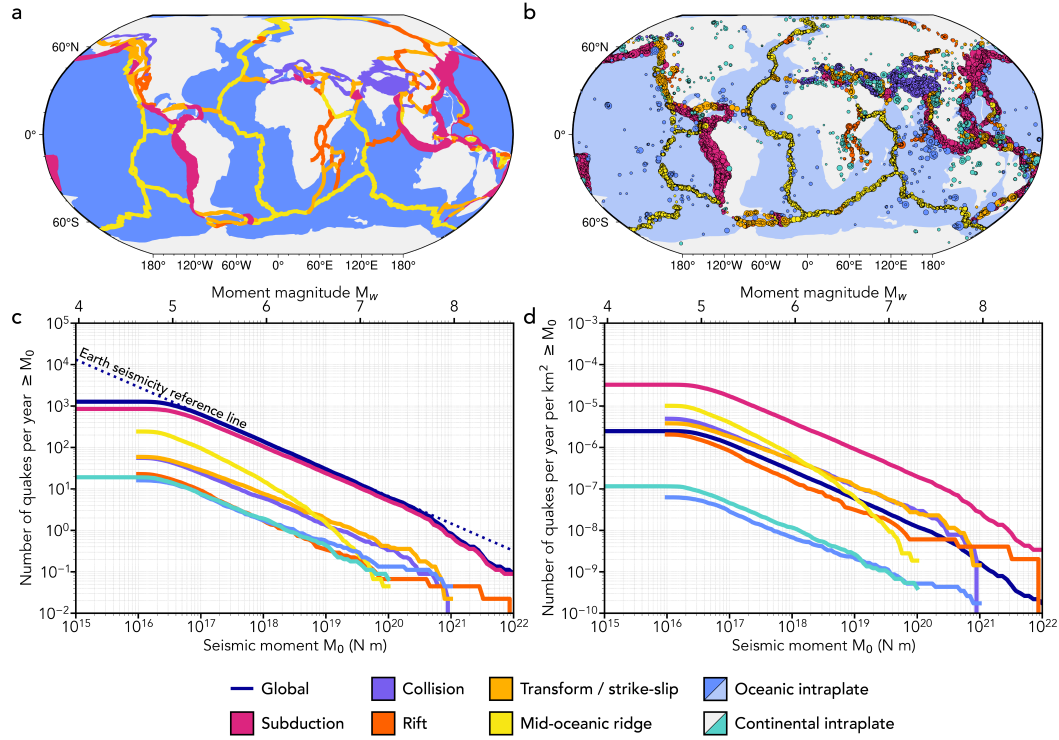


Figure 1. (a) Map of the Earth showing how its surface area is divided into seven discrete tectonic settings. (b) Earthquakes in the CMT catalogue from 1976 - 2020 coloured according to tectonic setting with the symbol size proportional to the earthquake magnitude. (c) Annual earthquake size-frequency distribution for the Earth based on the CMT catalogue and split into different tectonic settings. The dotted dark blue line is a reference line for Earth's seismicity extrapolated from the size-frequency distribution for seismic moments of 10^{17} N m to 10^{19} N m to lower and higher seismic moment assuming a constant slope (b -value). Note that this means that the Earth's reference line overestimates the amount of quakes with moment magnitudes larger than 8. (d) Seismicity density on the Earth for different tectonic settings, i.e., number of earthquakes in the CMT catalogue per year per km^2 . Maps are in Robinson projection.

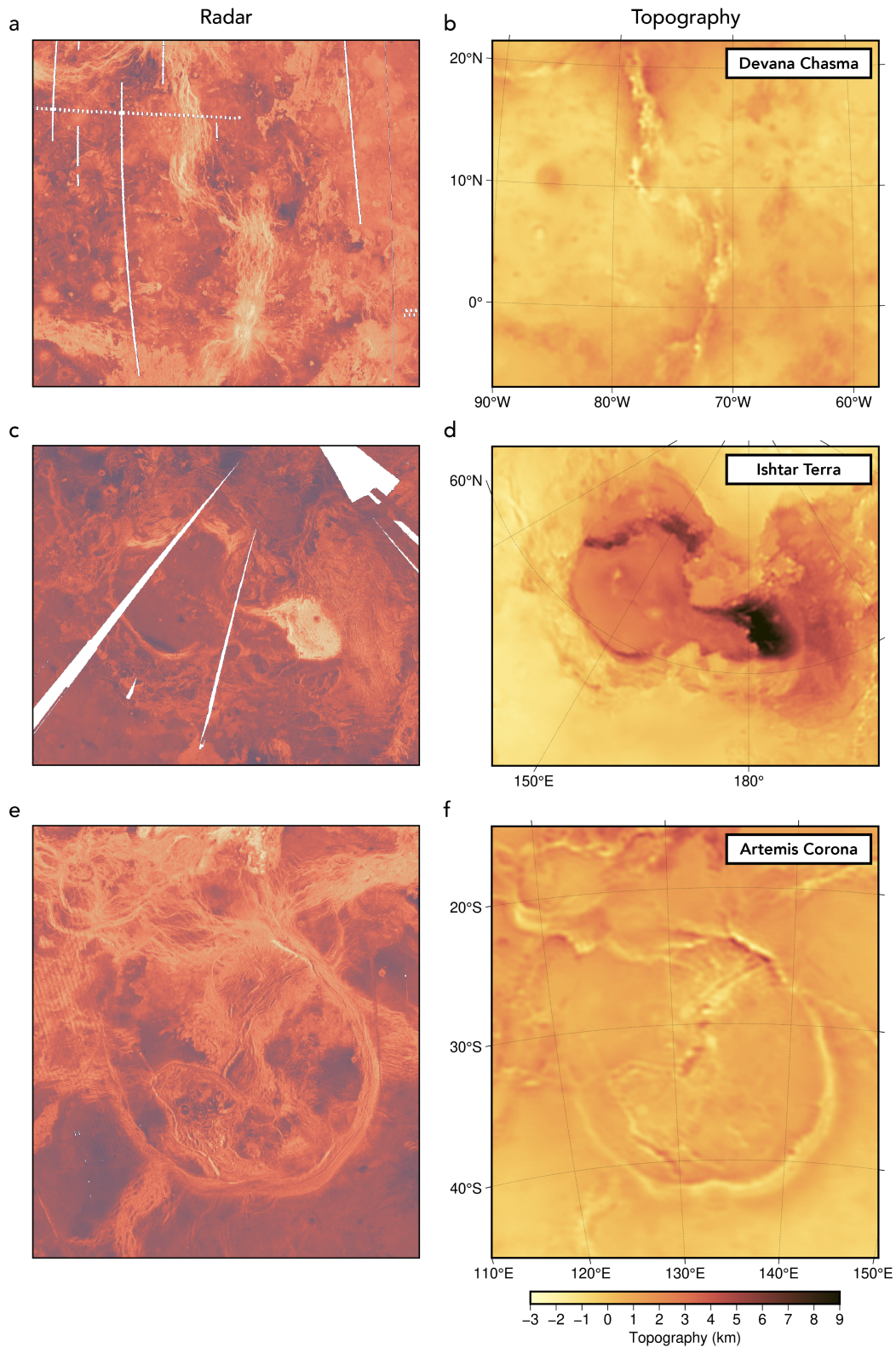


Figure 2. Examples of tectonic features on Venus with Magellan radar image mosaics on the left and topography maps derived from the Magellan altimetry data on the right. (a) Devana Chasma as an example of a rift system on Venus; (b) Ishtar Terra with Maxwell Montes as an example of a region characterised by compressional deformation and classified as a fold belt in this study following Price et al. (1996); (c) Artemis Corona, the largest corona on Venus. Maps are in Lambert azimuthal equal-area projection.

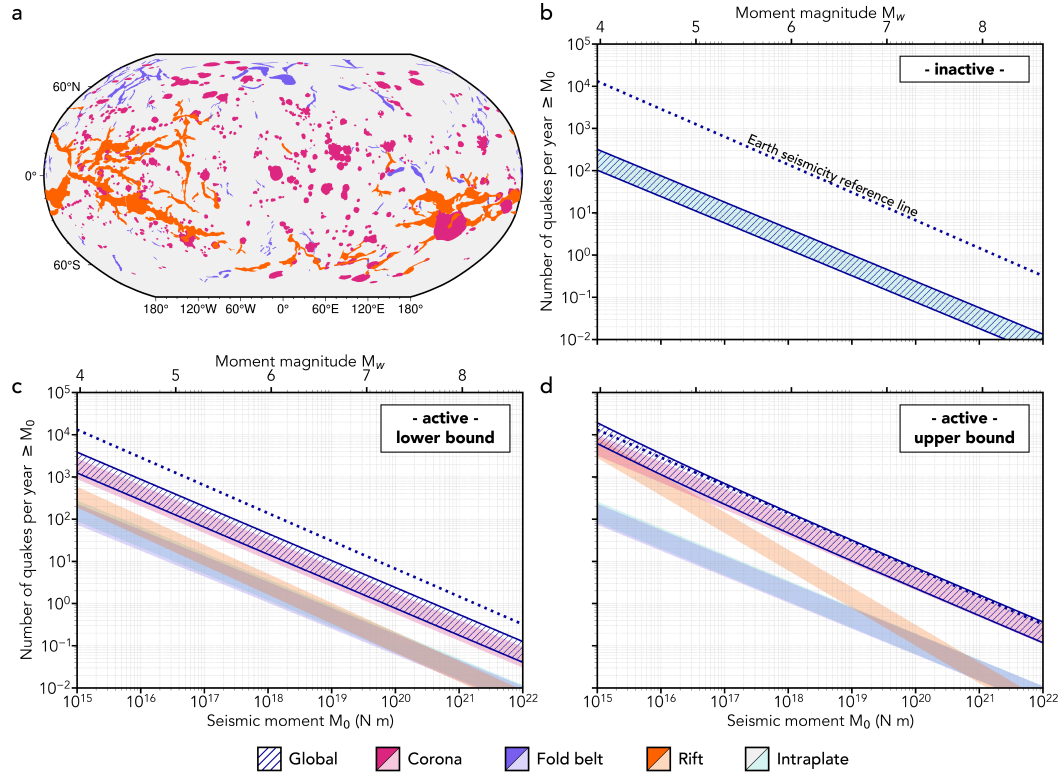


Figure 3. (a) Map of Venus (Robinson projection) showing the areas of mapped coronae, fold belts, and rifts (Price & Suppe, 1995; Price et al., 1996). (b-d) Ranges of potential quake size-frequency distributions on Venus for (b) an inactive Venus with background seismicity analogous to Earth's continental intraplate seismicity; (c) a lower bound on an active Venus; and (d) an upper bound on an active Venus. The hatched area shows the global, accumulated annual seismicity that combines the seismicity of the different individual tectonic settings. Note that because of the log-log scale, the global estimate and the seismicity range of the highest individual tectonic setting are closely-spaced. Dotted dark blue line indicates the reference Earth seismicity, which corresponds to the slope of the size-frequency distribution for seismic moments of 10^{17} N m to 10^{19} N m of global seismicity on Earth (Figure 1c).

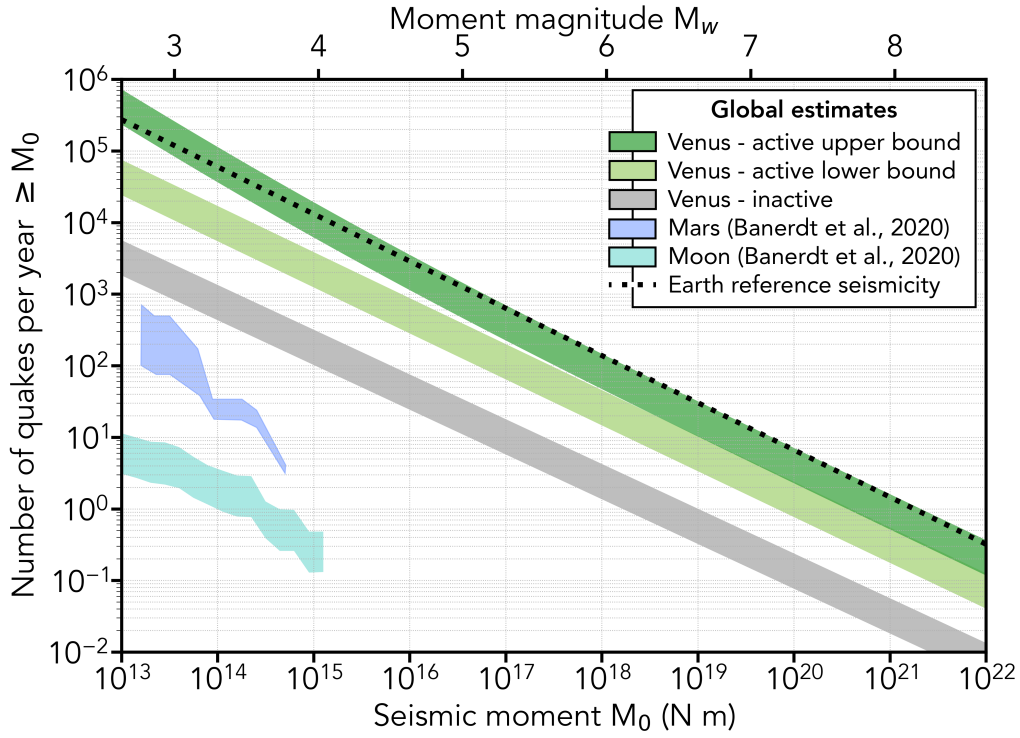


Figure 4. Summary of the global ranges of potential quake size-frequency distributions on Venus for our three end-member estimates from Figure 3. Global seismicity estimates for the Moon and Mars from Banerdt et al. (2020) are shown for reference. Dotted dark blue line indicates Earth’s seismicity for reference, which corresponds to the slope of the size-frequency distribution of global seismicity on Earth for seismic moments of 10^{17} N m to 10^{19} N m (Figure 1c).